DEVELOPMENT OF HIGH-THROUGHPUT AND ROBUST MICROFLUIDIC LIVE CELL ASSAY PLATFORMS FOR COMBINATION DRUG AND TOXIN SCREENING

A Thesis

by

HAN WANG

Submitted to the Office of Graduate Studies of
Texas A&M University
in partial fulfillment of the requirements for the degree of

MASTER OF SCIENCE

December 2011

Major Subject: Electrical Engineering

DEVELOPMENT OF HIGH-THROUGHPUT AND ROBUST MICROFLUIDIC LIVE CELL ASSAY PLATFORMS FOR COMBINATION DRUG AND TOXIN SCREENING

A Thesis

by

HAN WANG

Submitted to the Office of Graduate Studies of
Texas A&M University
in partial fulfillment of the requirements for the degree of

MASTER OF SCIENCE

Approved by:

Chair of Committee,	Arum Han
Committee Members,	Arul Jayaraman
	Byung-Jun Yoon
	Xing Cheng
Head of Department,	Costas N. Georghiades

December 2011

Major Subject: Electrical Engineering

ABSTRACT

Development of High-throughput and Robust Microfluidic Live Cell Assay Platforms for Combination Drug and Toxin Screening. (December 2011)

Han Wang, B.E., Tsinghua University, China

Chair of Advisory Committee: Dr. Arum Han

In both combination chemotherapy and environmental toxicology studies, characterizing effects of mixtures of drugs or toxins rather than simply analyzing the effects of single drugs or toxins are of significant interest. In order to determine such combination effects, it is necessary to systematically investigate interactions between different concentration-dependent components of a mixture. Conventional microtiter plate format based assays are efficient and cost-effective, however are not practical as the number of combinations increases drastically. Microfluidic live cell screening platforms can allow precise control of cell culture microenvironments by applying accurate doses of biomolecular mixtures with specific mixing ratios generated through integrated on-chip microfluidic gradient generators.

This thesis first presents a live cell array platform with integrated microfluidic network-based gradient generator which enables generation and dosing of 64 unique combinations of two cancer drugs at different concentrations to an 8 by 8 cell culture chamber array. We have developed the system into a fully automated microfluidic live cell screening platform with uniform cell seeding capability and pair-wise gradient

profile generation. This platform was utilized to investigate the gene expression regulation of colorectal cancer cells in response to combination cancer drug treatment. The resulting cell responses indicate that the two cancer drugs show additive effect when sequential drug treatment scheme is applied, demonstrating the utility of the microfluidic live cell assay platform.

However, large reagent consumption and difficulties of repeatedly generating the exact same concentrations and mixture profiles from run to run due to the fact that the generated mixture profiles have to rely on stable flow at optimized flow rate throughout the entire multi-day experiment limit the widespread use of this method. Moreover, producing three or more reagent mixtures requires complicated microchannel structures and operating procedures when using traditional microfluidic network-based gradient generators. Therefore, an on-demand geometric metering-based mixture generator which facilitates robust, scalable, and accurate multi-reagent mixing in a high-throughput fashion has been developed and incorporated with a live cell array as a microfluidic screening platform for conducting combination drug or toxin assays. Integrated single cell trapping array allowed single cell resolution analysis of drugs and toxin effects. Reagent mixture generation and precise application of the mixtures to arrays of cell culture chambers repeatedly over time were successfully demonstrated, showing significantly improved repeatability and accuracy than those from conventional microfluidic network-based gradient generators. The influence of this improved repeatability and accuracy in generating concentration specified mixtures on obtaining more reliable and repeatable biological data sets were studied.

DEDICATION

To my dear parents and family for your unconditional love and support

ACKNOWLEDGEMENTS

I would like to thank my advisor and committee chair, Dr. Arum Han, at the first place for his unwavering guidance and support all the way. Dr. Han has been an exceptional mentor, and given me invaluable encouragement and suggestions throughout my research. I would like to thank my committee members, Dr. Arul Jayaraman, Dr. Byung-Jun Yoon, and Dr. Xing Cheng for their advice and support. My special thanks go to Dr. Jayaraman for kindly providing me with the opportunity to work in his lab.

I would like to take the chance to thank my collaborator, Dr. Jeongyun Kim, for his patient tutorials and generous help. I also want to thank my group members, Jaewon Park, Huijie Hou, Hyunsoo Kim, Chiwan Koo, Osman Cifci, Celal Erbay, Siddharth Kumar and Adrian Guzman, and alumni Woosik Kim, Whitney Parker, and Jianzhang Wu for their enormous help in the lab and in life. The NanoBio Systems Lab is a wonderful place for research, and a warm family for life. It is my great honor to be part of it.

I am also grateful to my collaborators in the Translational Genomics Research Institute (TGen), Milana Cypert, Jianping Hua, and Mike Bittner for their generous help in providing the cell lines and drugs.

TABLE OF CONTENTS

CHAPTER Page

LIST OF FIGURES

Page

Page

CHAPTER I

INTRODUCTION

1.1. Combination Chemotherapy

Cancer cells are multigenic and can develop heterogeneity through the process of cell cycling, as well as the adaptive resistance to drugs that are targeting an individual molecule, leading to the loss of efficacy of conventional monotherapies. In some cases, the effectiveness of these monotherapies is further reduced due to the buffering effects of complex biological systems. In a complex disease system like cancer, multiple cellular activity pathways have been modified, thus it is natural to develop a strategy which attacks cancer in multiple aspects concurrently [1]. Therefore, researchers have adopted combination chemotherapy strategies where multiple agents with different mechanisms of actions are applied [2]. This kind of multi-target therapeutics can be more efficacious and less vulnerable to adaptive resistance.

Early development of combination chemotherapy was based on a simple assumption that the maximum therapeutic effect can be achieved by implementing each drug at its maximum tolerated dose (MTD). However, it has been revealed that the therapeutic effect of combination chemotherapy would largely depend on the dosage ratios of each drug in a combination, instead of their absolute doses [3]. This can be explained by the drug-receptor interaction theory, which is the basic principle underlining drug treatment. Drug induced effects are generally mediated by

---

This thesis follows the style of *Lab on a Chip*.

corresponding receptors, which can be described by the equation $[RD] = [R_T] \times [D] / (K_D + [D])$, where [RD] is the concentration of receptor-drug complex, $[R_T]$ is the total receptor concentration, [D] is the concentration of free drug (not bound to receptor), and K_D is the equilibrium dissociation constant for the binding of free drug D to free receptor R to form the RD complex, defined by the reaction $R + D \leftrightarrow RD$. Therefore, the dose and mixing ratios must be optimized to establish combination chemotherapy [4].

From the perspective of drug-receptor interaction theory, the drug combination can be classified as agonism (each drug binds and activates the receptor), antagonism (some drug only binds to the receptor but doesn't activate it), and inverse agonism (some drug binds and inactivates the receptor). With regard to the quantitative nature of combination effects, the drug combinations can be classified as additivity (combination effect equals the sum effect of individual drugs), subadditivity (combination effect is less than the sum effect of individual drugs), and superadditivity (combination effect is larger than the sum effect of individual drugs). A representative type of superadditivity, synergy, refers to the case in which each of the drugs exhibits its own effects and the effects of the combination are obviously greater. Synergy occurs in situations where either or both drugs in a combination have amplifying effects on the other.

1.2. Microfluidic Live Cell Assay

Live cell assays based on plastic culture plates (including microtiter plates) have been developed as tools for the characterization of the relationships between cell states,

environmental stimuli, and cellular responses. The three basic requirements of a live cell assay system are as follows [5]:

a) to maintain the viability of cell culture *in vitro* (subject);

b) to control the delivery and treatment of environmental stimuli (input);

c) to measure cellular response (output).

Conventional live cell assays are typically performed in culture flasks, petri dishes, and microtiter plates. These systems are extensively used due to cost efficiency, simplicity, standardized dimensions, automated equipments, and are gold standards for live-cell assay. However, these methods suffer from large reagent consumption, low throughput, time-consuming procedures, and labor-intensive operations. Automatic pipetting systems can overcome the limitations of low throughput, extended time length, and manual intervention, however are generally costly and not commonly available. Also, these conventional methods have difficulties in mimicking *in vivo-like* cell microenvironments *in vitro*[6].

As an emerging technology, microfluidics enables precise and flexible control of cell microenvironments at the micro- and submicrometer scale. Microfluidic systems allow manipulating extremely small amount of samples and reagents with high precision. Laminar flow arises as the dominant flow transportation method in microfluidic devices due to low Reynolds number, which facilitates spatially controlled reagent delivery. Furthermore, the small dimensions of microfluidic components such as microvalves, micropumps, microreactors, gradient generators, and multiplexers and the ability of high level integration of such functional components enable building a

complete live cell culture and assay platform on a single chip, so called “lab-on-a-chip”, or “micro total analysis systems” (μTAS). Various microfluidic live cell assay systems have been developed in the past decade, including devices that allow differential treatment of sub-cellular regions of a single bovine capillary endothelial cell by multiple laminar flow [7], long-term culture and monitoring of extremely small populations of bacteria with single cell resolution in a microchemostat array [8], continuous perfusion of humane carcinoma (HeLa) cells with repeated cell growth/passage cycles [9], and continuous separation of blood plasma utilizing the pinched flow fraction scheme [10]. These examples show the capability and potential of microfluidic and lab-on-a-chip platform for cellular assays and studies.

Microfluidic devices have been fabricated in silicon, glass, and a wide range of polymers. The development of soft lithography [11], a series of techniques where elastomeric devices can be replicated from a single master mold repeatedly, has proliferated the development and usage of microfluidic devices and systems to the broader life science community. This method is cheap, more accessible to general researchers, capable of patterning non-planar and 3D structures, and compatible with a variety of polymers such as elastomers. Poly(dimethylsiloxane) (PDMS) has been generally used for its transparency, gas permeability, biocompatibility, and surface properties. The cast molding fabrication procedure goes as following: the master is prepared by photolithography, hot embossing, or other techniques; and then PDMS base and curing agent are mixed and poured onto the master; then the PDMS mixture is cured by heat, released from the master, and bonded to glass or other substrates by oxygen

plasma treatment. Pieces of partially cured PDMS blocks can also be bonded by attaching them together and fully curing the system.

1.3. Microfluidic High-throughput Screening Systems

Over the past twenty years, technological advancements in automation and miniaturization as well as economic pressures have driven rapid development of high-throughput screening (HTS) techniques. HTS has been established as the main technique for toxicology research and drug discovery in pharmaceutical companies as well as in research laboratories. Typical HTS systems can perform over 10,000 assays per day, while ultraHTS (uHTS) systems can perform over 100,000 assays per day. The ever increasing need for HTS stems from the growing number of potential therapeutic molecular targets emerging from functional genomic studies as revealed by the human genome program, and the rapid development of large compound libraries derived from parallel and combinatorial chemical synthesis techniques [12]. Solution-based HTS is the primary step to identify the potential lead, which is capable of modulating target biochemical molecules from a large library of compounds. Cell-based HTS aims to build integrated platforms that enable automated monitoring of molecular processes within cells (e.g. gene expression modulation) and cell functionality changes (e.g. apoptosis), as well as to facilitate target validation and lead optimization. The earlier cell-based HTS assays are applied in the drug development cascade, the better quality of leads can be identified with reduced lead failures.

Miniaturization of HTS has scaled down the conventional petri dish into 96-well, 384-well, and 1536-well microtiter plate formats, and automatic plate reader has been developed to quantitatively analyze the screening data in a high-throughput fashion. This microtiter based HTS technique benefits from standardized dimensions and compatibility with laboratory automation instruments, and has been accepted as the standard approach in chemistry and biology fields. However, further miniaturization of microtiter plates turned out impractical due to expedited medium evaporation, increased surface-to-volume ratio, and increased surface tension. Furthermore, this method is inefficient in delivering temporarily and spatially varying stimuli, controlling cell position and local density, thus giving rise to the need for next generation HTS techniques [5].

Microfluidic live cell assay platform holds the potential as next generation HTS technology for its precise and flexible control capability of cell microenvironment, capability of dynamically controlled cell and fluid delivery dynamically over time, reduced reagent volume, capability of automation, multi-functionality, and scalability.

Wang, *et al.*, developed a 24×24 sieve embedded circular chamber microfluidic cytotoxicity array which could test six distinct cell lines with twelve toxins formulations [13]. Cell seeding channels were orthogonal to toxin injection channels, and within each channel intersection was a circular chamber with cell-trapping sieves. This 576-chamber microfluidic array was used to screen three cell types (BALB/3T3, HeLa, and bovine endothelial cells) against a panel of five toxins (digitonin, saponin, CoCl2, NiCl2, acrolein) by fluorescence microscopy to demonstrate its functionality.

Lee, *et al.*, developed an addressable 8×8 array of cell culture chambers with an integrated microfluidic gradient generator to observe the serum response of HeLa human cancer cells in 64 parallel cultures [14]. Each cell culture chamber was designed with a ‘‘C’’ shaped ring to effectively decouple the central cell growth regions from the outer fluid transport channels. This microfluidic device overcame major problems in multiplexing nanoliter culture environments by enabling uniform cell loading, eliminating shear and pressure stresses on cultured cells, providing stable control of fluidic addressing, and permitting continuous on-chip optical monitoring.

1.4. Microfluidic Single Cell Assay Platforms

In recent years, single cell level analysis has drawn significant interest in comparison to conventional population based cell group analysis [15]. Single cell assay not only pushes the resolution to an individual cell level, but also offers enormous potentials in studying cell heterogeneity and individual cell behaviors, such as cell growth, differentiation, and apoptosis. Also single cell assay opens the window of studying sub-cellular activities and molecular processes more directly. Moreover, the isolation of individual cells provides quantitative information on the heterogeneous behaviors of individual cells not obtainable through population-based studies.

Microfluidic systems are ideal methods for single cell assay due to their exquisite capability for manipulating small volume of samples down to single cells, and have been used for applications such as single cell microinjection where single cells were directed to a fixed microneedle [16], counting low-copy number proteins in a single cell by

manipulating, lysing, labeling, and quantifying the protein content of a single cell [17], and monitoring single cell secretion in real-time with confocal microscopy [18].

Single cell trapping enables easy tracking/analysis of single cell level gene expression. Various microfluidic single cells trapping schemes have been demonstrated, such as hydrodynamic trapping with physical obstacles, or trapping with applied external forces such as dielectrophoresis (DEP), magnetic field, and acoustic waves [19]. Hydrodynamic trapping of individual cells with physical obstacles offers a simple, effective, and physiologically favorable solution for isolating single cells in a high-throughput manner. Di Carlo, *et al*. has developed a large scale single cell trapping array with raised trapping structures for studying dynamic cell growth and division on chip [20]. A derivative of this trapping scheme will be implemented into our developed high-throughput single cell environmental toxin screening platform integrated with geometric metering-based concentration mixture generator to allow quantitative single cell resolution toxin treatment analysis.

1.5. Organization of the Thesis

The thesis will describe the development of high-throughput and robust microfluidic live cell combination screening platforms, including the designs and working principles, fabrication, and experimental results.

Chapter II will present a microfluidic network-based gradient generator device used for high-throughput screening of the combination gene regulations of HCT116

colorectal cancer cells with two cancer drugs. A design of two pair-wised gradient generators with integrated cell culture array will be demonstrated.

A novel geometric metering-based mixture generator and fluid delivery scheme for on-demand combination environmental toxin mixture generation and exposure on hepatoma cells will be demonstrated in Chapter III. This innovative approach overcomes limitations of conventional networked-based gradient generator in multiple aspects and enables robust and scalable multi-reagent mixture generation by "hardware programming". The pressurized membrane pumping (PMP) method enables robust and accurate fluid delivery in the microfluidic cell culture system.

Chapter IV will summarize the thesis and give the directions and plan for future research of the developed platform.

CHAPTER II

MICROFLUIDIC NETWORK-BASED LIVE CELL COMBINATION DRUG SCREENING PLATFORM

2.1. Introduction

Laminar flow phenomena in microfluidics allows the generation of fluidic gradients, which can then be used to generate mixtures of two reagents at various concentrations. The most widely used microfluidic gradient generator is the network-based gradient generator as in the configuration of series of serpentine channels which can generate spatially and temporally constant gradient profiles by repeatedly splitting, mixing and combining inlet fluids [21]. Since the first introduction by Jeon, *et al.*, this kind of network-based gradient generator and its derivatives have won great popularity due to its simplicity of operation, capability of generating predictable, and complex gradient profiles, and adaptability to general settings [22, 23]. Figure 2.1 shows a simple microfluidic gradient generator demonstrating the generation of 8 different concentrations of color dye using series of splitting, mixing, and combining microfluidic channel network. In this particular example, 8 different concentration combinations are generated automatically by simply pushing blue dye (inlet A) and red dye (inlet B) into the two inlets at equal speed. This gradient profile can be adjusted by varying relative flow rates of the two inlet solutions, and more complex gradient profiles can be achieved by adding more inlets or apply complex control schemes. Using this concept, linear, logarithmic, and arbitrary concentrations of chemicals have been generated by various

researchers. More complex profiles can also be achieved by introducing multiple inlets [23]. Concentration gradient profiles can be calculated through an analogy with an equivalent electrical circuit model [22].

Our microfluidic live cell assay platform utilizes the basic gradient generation scheme shown in Figure 2.1, and spatially and temporally constant gradients can be generated at stable flow rates of inlet solutions.

2.2. Design and Fabrication

This design used here is adopted from the microfluidic platform initially developed by our collaborator Kim *et al.* [24]. The high-throughput combination drug screening platform consists of two orthogonally positioned microfluidic network-based gradient generators and an array of 64 cell culture chambers (chamber size: 700 μm × 700 μm) with four symmetric cell-seeding ports (Figures 2.2 & 2.3). Two gradient microvalves control the opening/closure of both gradient generators, respectively. The two chamber microvalves control the cell culture chamber array in two orthogonal directions. By actuating the gradient microvalve with chamber microvalve in the same direction, cells trapped inside the culture chambers can be exposed to the chemical gradient from one gradient generator while isolated from the chemical gradient of the other gradient generator. The drug exposure profile after exposing the cell culture

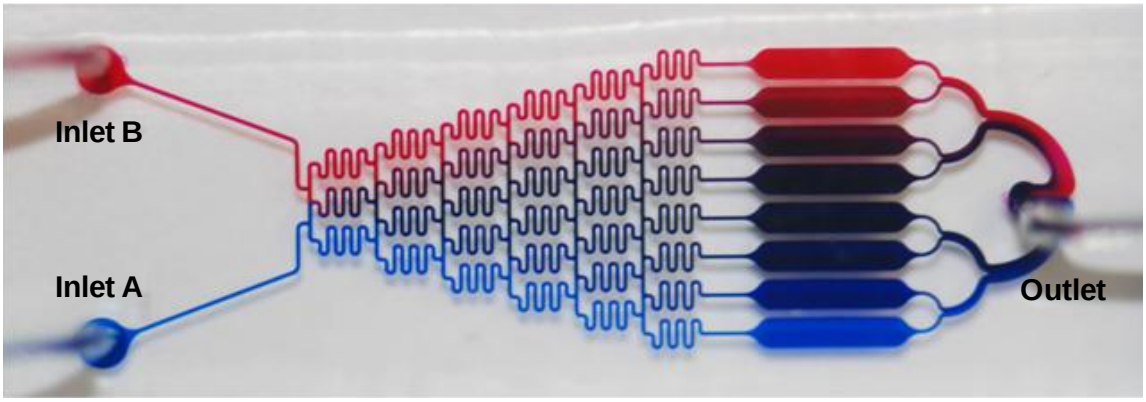

Figure 2.1. A microfluidic network-based gradient generator.

chambers with gradient of drug B was simulated by color dyes as shown in Figure 2.3(A). Together with the second gradient generator for drug A, this configuration allows the 64 cell culture chambers to be exposed to 64 different combinations of drugs A and B at 8 different dilutions each sequentially in a single experimental run. Figure 2.3(B) shows an individual cell culture chamber with HCT116-MKI67-1000 GFP colorectal cancer cells cultured inside.

This microfluidic device has been previously used in a study lead by our collaborator Kim *et al.* to probe the combinational effects of doxorubicin and TNF-related apoptosis-inducing ligand (TRAIL) on PC3 prostate cancer cells [24]. We have further developed this microfluidic platform to overcome previous limitations in full automation capability and non-uniform cell seeding that influences the reliability of the on-chip assays. First, a LabVIEW^{TM} interface was developed to control the microfluidic valve actuation and drug injection by controlling 4 pneumatic actuators and 2 syringe pumps simultaneously. This enabled fully automated multi-day sequential cancer drug assay with periodic medium and drug replenishment (Figure 2.2). To overcome non-uniform cell seeding in each of the 64 cell culture chambers, four symmetric cell seeding ports connected to the cell culture chamber array was developed. Together with the two outlets, this symmetric cell seeding scheme reduced the sidewall effect of single seeding port scheme, where much lower density of cells can be found near the channel sidewalls.

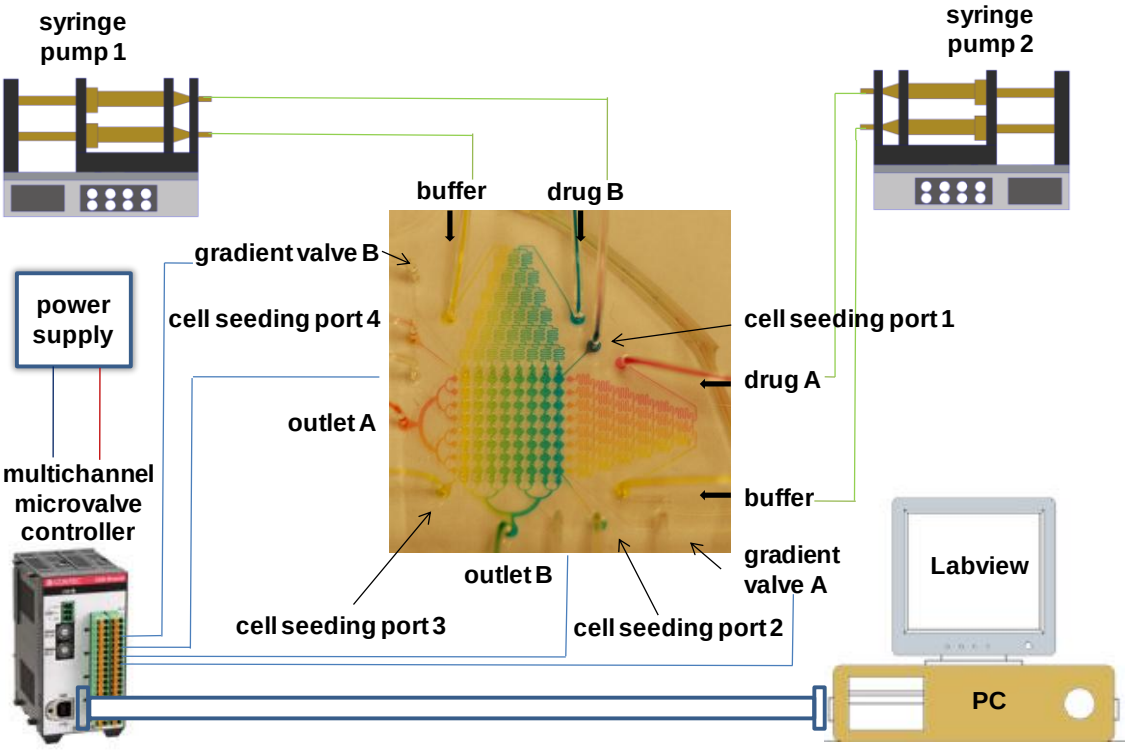

Figure 2.2. Schematic diagram of the high-throughput combination drug treatment live cell array experimental setup. A LabVIEW™ interface controlled a multichannel microvalve controller and syringe pumps, enabling fully automatic multi-day drug treatment assays.

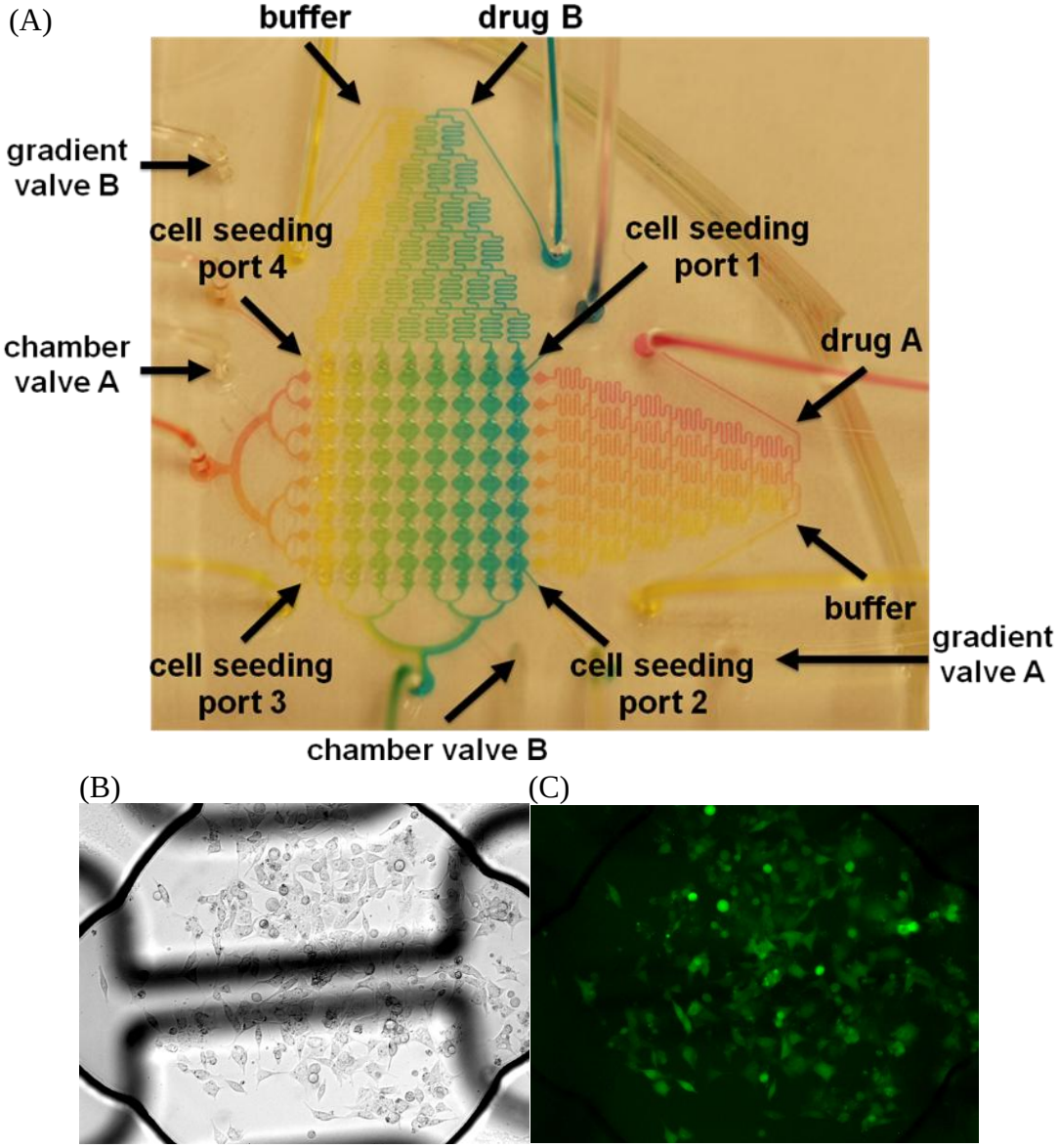

Figure 2.3. Images of the high-throughput live cell array microdevice for combination drug treatment assay. (A) Array of 8 by 8 cell culture chambers (chamber size: 700 μm × 700 μm) are exposed to 64 pair-wise combinations of drugs A and B at different dilutions. (B) Brightfield (left) and fluorescence (right) images of HCT116-MKI67-1000 GFP reporter colorectal cancer cells inside one of the cell culture chambers.

The microfluidic platform is composed of two layers, the pneumatic control layer which contains pneumatic valves, and the fluidic layer which contains fluidic channels. The pneumatic valves used here are the normally closed microvalves. Figure 2.4 shows the schematic of the normally closed valve. When positive pressure was applied, the membrane in the valve region was bent down and the fluidic channels were blocked; on the contrary, when negative pressure was applied, membrane in the valve region was bent up and the fluidic channels were connected. In natural state the membrane tends to bend down due to its elasticity, where positive pressure can be reduced or even removed if no fluid transportation is needed. This scheme is especially suitable for cell culture and cell assay since the need for large pressure during incubation is eliminated, significantly reducing bubble generation during valve operation.

The microfluidic cell culture platform was fabricated with poly(dimethylsiloxane) (PDMS, Sylgard 184, Dow Corning) using soft lithography [11] (Figure 2.5). The soft lithography master molds for the microfluidic device were fabricated with standard photolithography processes. For the fluidic layer, the silicon

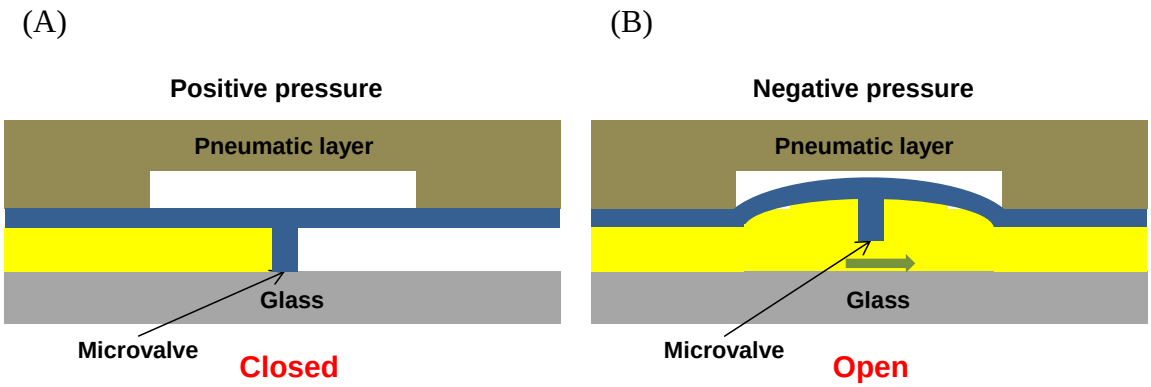

Figure 2.4. Schematic of the normally closed valve. (A) When positive pressure is applied, the membrane in the valve region is bent down and the fluidic channels are blocked. (B) When negative pressure is applied, membrane in the valve region is bent up and the fluidic channels are connected.

wafer was rinsed with acetone and IPA, and heated at 150°C for 10 min on a hot plate to vaporize the liquid, then negative photoresist SU-8 2050 (Microchem) was spincoated at 1800 rpm for 50 sec, soft baked at 65°C for 20 min and 95°C for 40 min, exposed at the dosage of 220 mJ/cm^2, yielding a 100 μm thick fluidic layer pattern. For the pneumatic layer, the silicon wafer was rinsed with acetone and IPA, and heated at 150°C for 10 min on a hot plate, then negative photoresist SU-8 2050 (Microchem) was spincoated at 800 rpm for 50 sec, soft baked at 65°C for 40 min and 95°C for 40 min, exposed at the dosage of 330 mJ/cm^2, yielding a 200 μm thick fluidic layer.

Thereafter PDMS prepolymer and curing agent were prepared at 10:1 weight ratio, and degassed in a vacuum chamber for 1 h. The control layer was casted to 5mm think, while the fluidic layer was spincoated at 700 rpm for 30 sec, yielding a 150 μm thick membrane. After curing in an 80℃ oven for 2 h, the control layer and fluidic layer were bonded with oxygen plasma treatment (100 mTorr, 100W, 40 sec) by visual alignment. The PDMS microfluidic device was finally bonded on a glass substrate with oxygen plasma treatment (100 mTorr, 100W, 40 sec).

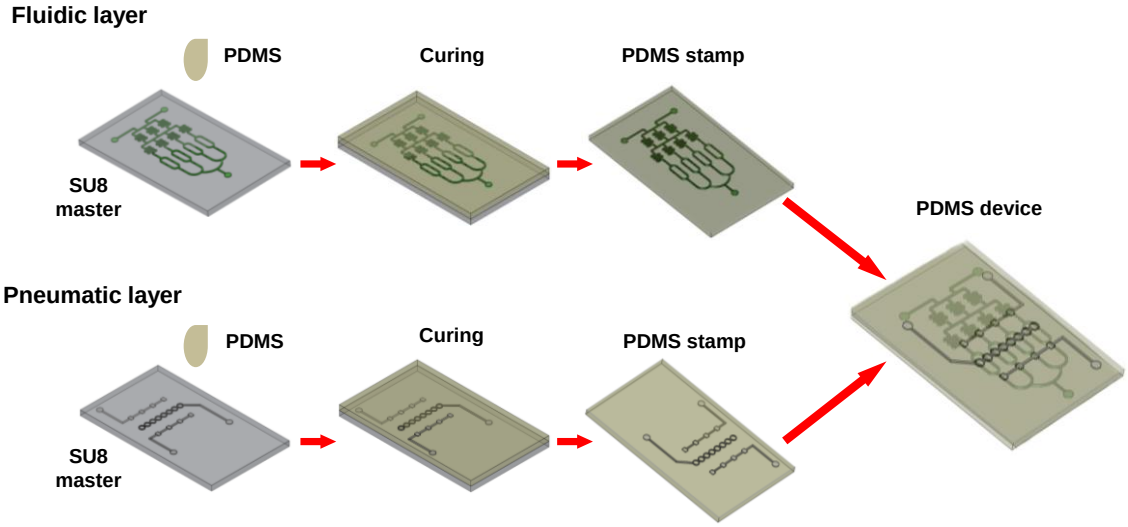

Figure 2.5. Illustration of the soft lithography process.

2.3. Experimental

The HCT116-MKI67-1000 GFP cell line was obtained from Translational Genomics Research Institute (Phoenix, AZ), and maintained with RPMI 1640 medium (Invitrogen) supplemented with 10% fetal bovine serum (FBS, Invitrogen) in a 5% CO_2 humidified incubator at 37℃. Prior to microfluidic experiment, the cells were trypsinized and stained with Vybrant® Dyecycle™ violet live cell nuclei stain (Invitrogen) at 5 μM for 30 min as instructed.

The assembled PDMS microfluidic device was thereby sterilized with UV, and coated with Collagen I (Invitrogen) to enhance cell attachment to the glass substrate. Cells were trypsinized, stained, and seeded via the four symmetric cell-seeding ports simultaneously with the syringe pump. After 4 h of incubation to allow cells to settle down, phenol red-free and low riboflavin content culture medium M-199 (Invitrogen) supplemented with 10% fetal bovine serum (FBS) was refreshed every 4 h for 24 h, at 5 μl/min flow rate for 3 min each time. The phenol red-free and low riboflavin content culture medium was used to decrease background noise for fluorescence microscopy. This initial incubation time was then followed by sequential treatment with dilution gradients of two drugs Lapatinib and LY 294002 (LC Laboratories) using the same refreshing scheme for a total exposure time of 48 h. The highest concentration of Lapatinib was optimized to 16 μM, while LY 294002 to 25 μM.

Brightfield and fluorescence images were acquired with a Zeiss 200M inverted microscope using an AxioCam MRM Rev 2 camera (Carl Zeiss). Thereafter

fluorescence images were analyzed with ImageJ (NIH). The green fluorescent (GFP) channel was analyzed by measuring the sum of fluorescence intensity per cell area, while the blue fluorescence channel showing nuclei was analyzed by counting cell numbers.

2.4. Characterization of Cell Seeding Uniformity

The four-port symmetric cell-seeding design improved the uniformity of cell seeding in the microfluidic device, which is an important parameter in parallel comparison studies. Figure 2.6 shows images of cell culture chambers after seeding with the four symmetric port design (Figure 2.6(A)) and the single seeding port design (Figure 2.6(B)) at three different locations of the microdevice; near the seeding port (Figure 2.6 left images), near the center of the culture chamber array (Figure 2.6 middle images), and near the opposite position of the seeding port (Figure 2.6 right images). Three chambers in above mentioned locations were picked up and compared for cell seeding uniformity. It can be clearly seen that the four symmetric seeding port scheme greatly enhanced cell seeding uniformity, with a uniform cell seeding density of 173 ± 5.9 cells/chamber (C.V. = 3.4%) compared to 122 ± 51 cells/chamber (C.V. = 41.8%) as in the device with only one cell seeding port throughout the 64 cell-culture chambers.

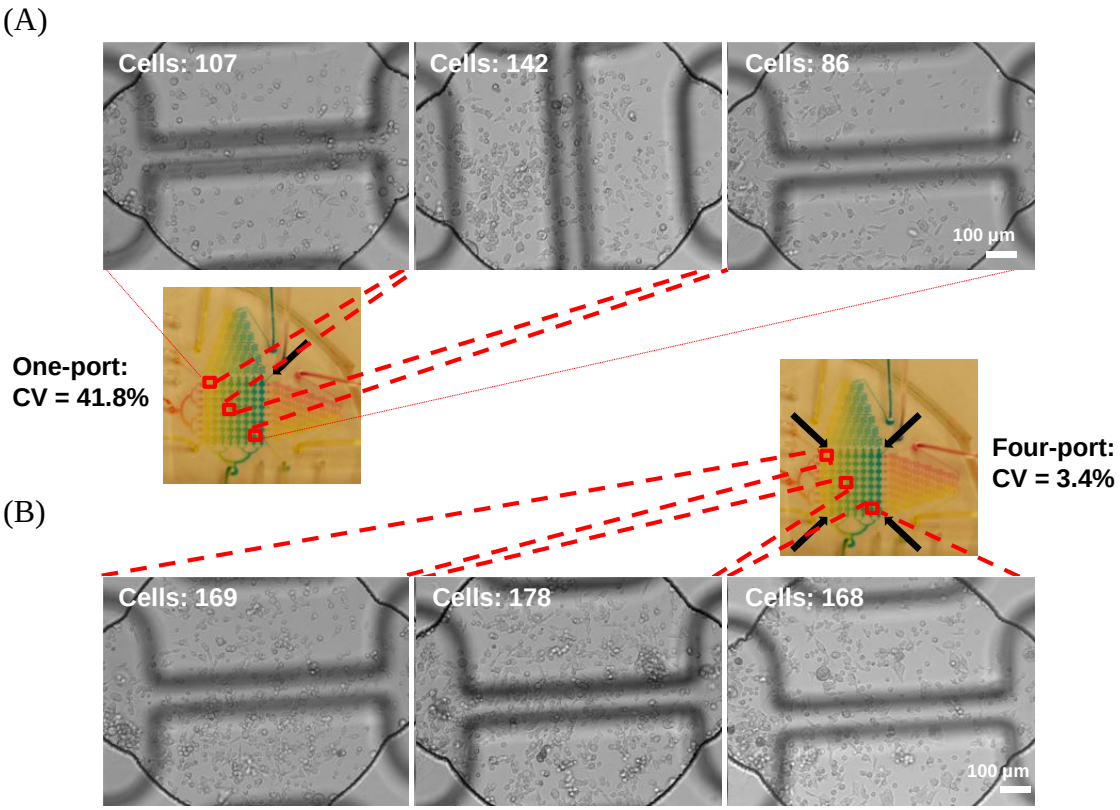

Figure 2.6. Improved cell seeding uniformity with symmetric seeding scheme design. (A) Selected images of cell culture chambers at different locations showing non-uniform cell seeding with one seeding port. (B) Selected images of cell culture chambers at different locations showing uniform cell seeding with four symmetric seeding ports. The arrays indicate cell seeding ports.

2.5. Drug Effectiveness Analysis

The microfluidic high-throughput screening platform was used to investigate the gene regulations of HCT116 colorectal cancer cells through combination therapies of cancer drug Lapatinib and kinase inhibitor LY 294002 in the sequential treatment fashion.

The effectiveness of the drug treatment was analyzed in two different ways: 1) the inhibition of the proliferation using the MKI67-GFP promoter-reporter as an indicator of the proliferative activity and 2) the suppression of cell growth overtime.

2.5.1. Drug Treatment Analysis through GFP Expression

In the first method, green fluorescence images were acquired and the sum of fluorescence intensity per cell area was measured with ImageJ. The sum instead of the mean value of fluorescence intensity within each cell area was used in consideration of more accurately representing the total GFP expression status for each cell. Since the cells are highly heterogeneous in a culture group, they differ significantly in cell shape, size, and cell cycle stages. Therefore the sum of fluorescence intensity per cell area can be a more accurate representation of the total GFP reporter activity inside a cell than purely calculating the average fluorescence intensity. Figure 2.7 shows the effectiveness of Lapatinib in reducing the proliferative activities of HCT116 cells using GFP reporter in the microdevice. With the increasing concentration of the drug Lapatinib from 0 to 16 μM, the total intensity of the green fluorescent signal decreased by 50%, indicating

reduced proliferative activity. The IC50 was 16 μM. The result demonstrates efficacy of Lapatinib in reducing the proliferation, as well as the utility of using the microdevice in this cancer cell drug assay. The result using the microfluidic platform was verified using a conventional 96-well plate study. For the 96-well plate experiment, HCT116 cells were seeded at 5E5 cells/ml, cultured for 12 h with M199, and then treated with different concentrations of Lapatinib for 48 h. Figure 2.8 compares the result from the microfluidic platform to that of the 96-well plate, with Y-axis indicating the decrease in fluorescence intensity in response to increasing concentrations of Lapatinib. Although some deviation was observed when comparing the microdevice result to the 96-well plate result, the general trend as well as IC50 matched well in both approaches, indicating the utility of the microdevice. The deviations might come from the differences in cell culture environments, and effective drug concentration in these two platforms.

(A)

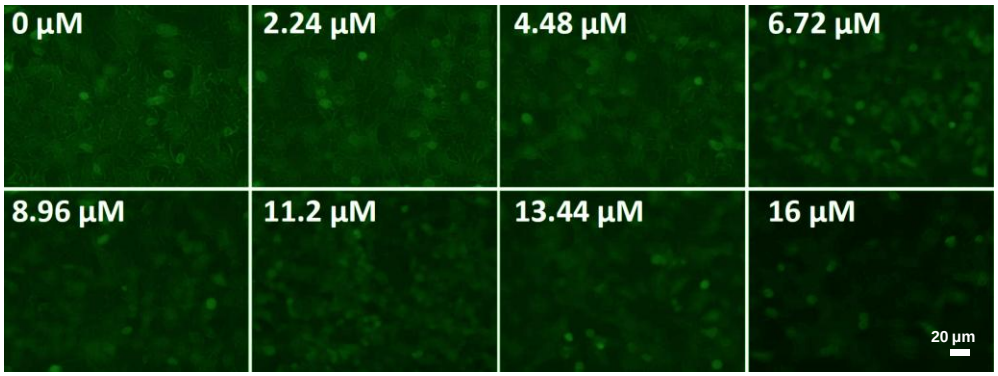

(B)

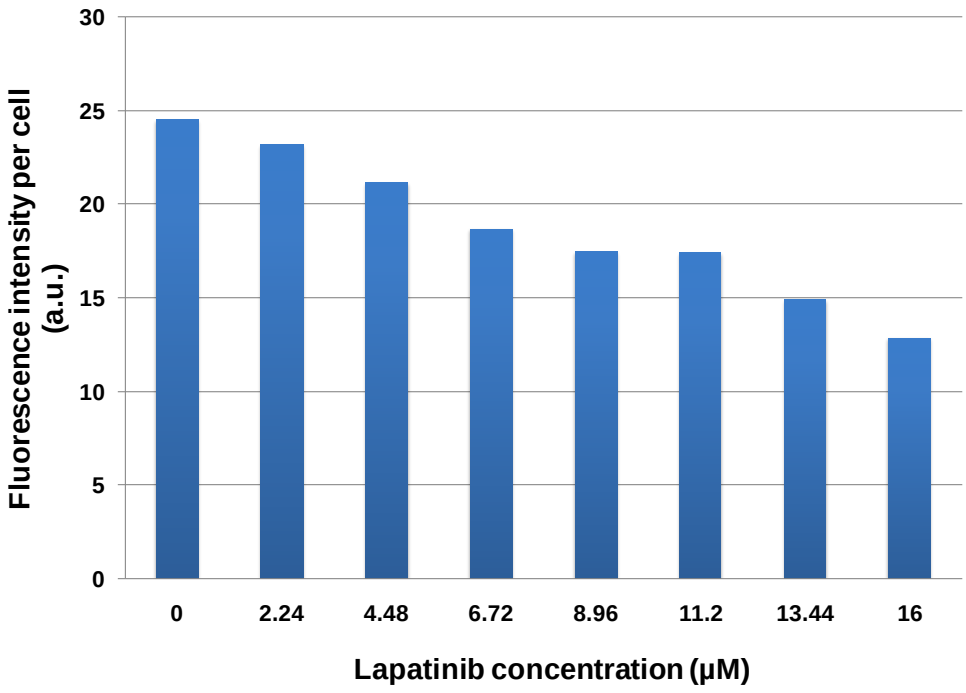

Figure 2.7. The efficacy of Lapatinib in reducing the proliferation activity of HCT116 cells tagged with GFP reporter. (A) Fluorescence images of the HCT116-MKI67-1000 GFP cells after 48 h of Lapatinib treatment at 8 different concentrations. (B) The sum of fluorescence intensity per cell area versus Lapatinib concentrations. The drop in fluorescence intensity indicates the effectiveness of the drug.

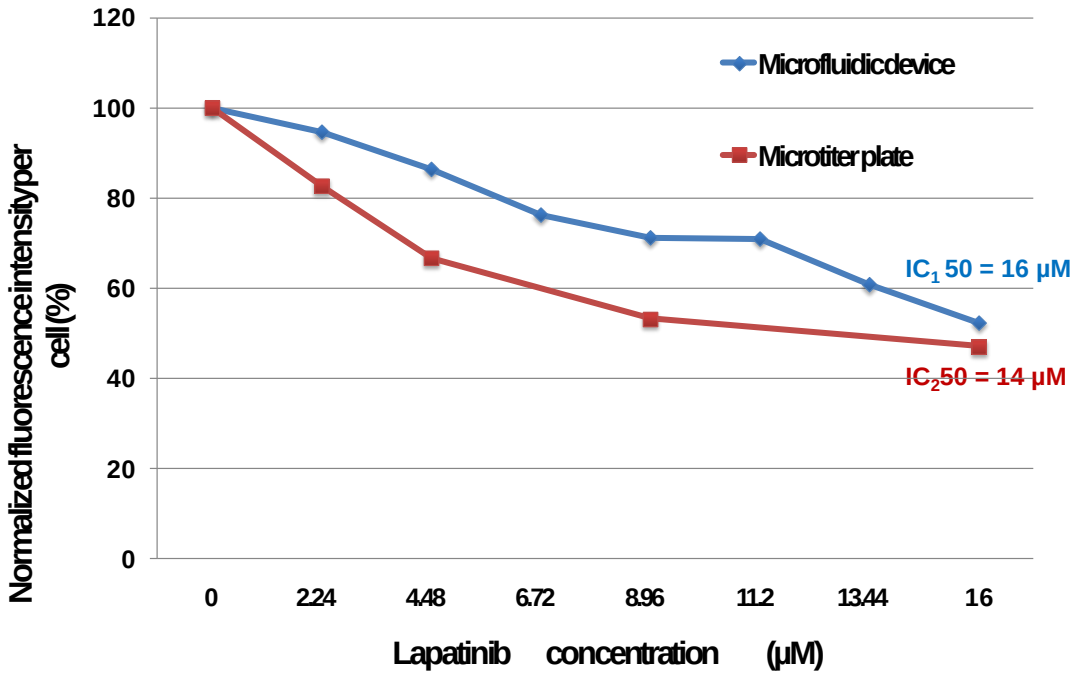

Figure 2.8. Fluorescence intensity fold change of the HCT116-MKI67-1000 GFP cells in both microfluidic device and microtiter plate after 48 h of Lapatinib treatment at 8 different concentrations.

2.5.2. Individual Drug Treatment Analysis through Cell Growth Analysis

The fluorescence signal from the GFP expression in HCT116 cells was extremely weak and the signal to noise ratio was only around 5. This caused major problem in measuring the fluorescence intensity drop induced by drug treatment. Therefore we developed an alternative method by monitoring cell growth rate change based on our observation. In this method, cell growth rate change in response to different concentrations of Lapatinib and LY 294002 as well as combinations of these two drugs was analyzed. Blue fluorescence images showing nuclei were acquired, and cell growth rates were calculated from the ratios of cell numbers in each chamber before and after drug treatment over 48 h. Figure 2.9(A) and (B) show the normalized cell growth rate changes due to exposure to concentration gradients of Lapatinib and LY 294002. In Figure 2.9(A), the cell growth rate decreased from 100% to 34% when exposed to 24 μM of Lapatinib. In Figure 2.9(B), the cell growth rate decreased from 100% to 21% when exposed to 25 μM of Lapatinib. The IC50 for cell growth change with Lapatinib was 14 μM, while the IC50 with LY 294002 was 20 μM. These results indicate the significance of cell growth activity affected by the application of the two drugs, which can be used as an indicator of the drug effectiveness.

(A)

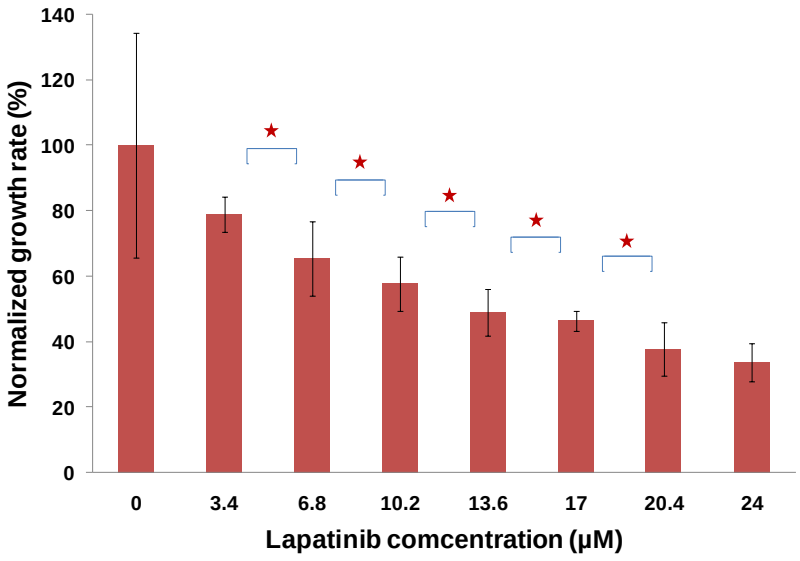

(B)

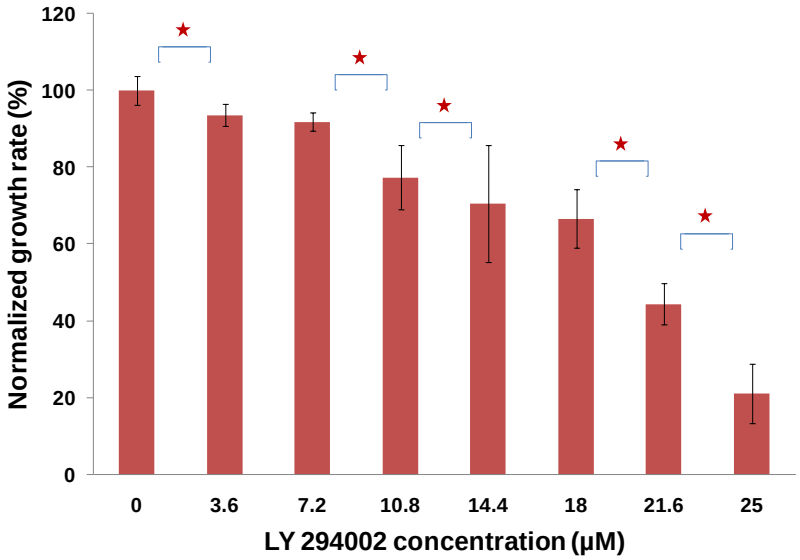

Figure 2.9. The growth rate change of HCT116 cells exposed to Lapatinib and LY 294002 at concentration gradients. (A) Cell growth rate change after 48 h of Lapatinib treatment at different concentrations (★, $p < 0.05$). Sample size $n = 5$. (B) Cell growth rate change after 48 h of LY 294002 treatment at different concentrations (★, $p < 0.05$). Sample size $n = 7$.

To validate the usage of cell growth monitoring with nuclei staining as an indicator of the drug efficacy, a comparison between GFP reporter expression and cell growth rate was performed. Figure 2.10 compares cell responses to different concentrations of Lapatinib in terms of reduction in GFP intensity per cell and in terms of reduction in cell growth rate. The two curves closely followed each other both in the trajectory and in the final effect, and the correlation coefficient of the growth rate change and fluorescence intensity change was 0.9921. This strong correlation suggests that cell growth rate measurement can be used as a supplementary or alternative method in drug efficacy analysis.

2.5.3. Combination Drug Treatment Analysis through Cell Growth Analysis

Based on the previous individual drug treatment analysis through cell growth rate monitoring, the utility of this growth rate analysis method was proved. Therefore the combinational effect of Lapatinib and LY 294002 treatment was analyzed only using cell growth analysis so far as shown in Figure 2.11. In this figure, Lapatinib alone (LY 294002 concentration = 0 μM) caused 32.6% drop of HCT116 growth rate, while LY 294002 alone (Lapatinib concentration = 0 μM) caused 76.5% drop of growth rate. The added total effect of Lapatinib and LY 294002 is 109.1%, which is larger than 100%. In combination, the maximum effect of the two drugs used together (Lapatinib concentration = 16 μM, and LY 294002 concentration = 25 μM) was 92%, suggesting that Lapatinib and LY 294002 are agonists and have additive effect when used together.

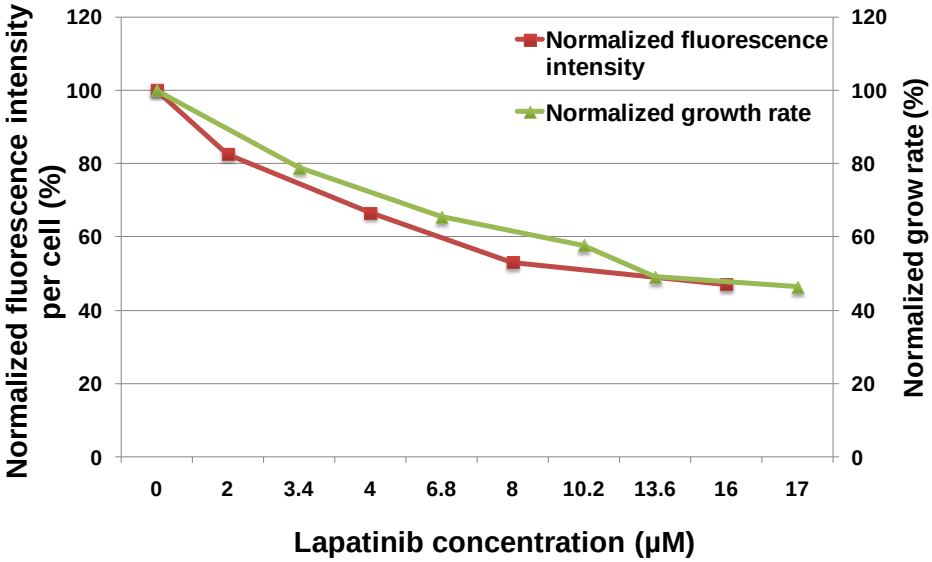

Figure 2.10. The correlation of fluorescence intensity change and growth rate change in response to Lapatinib gradient treatment.

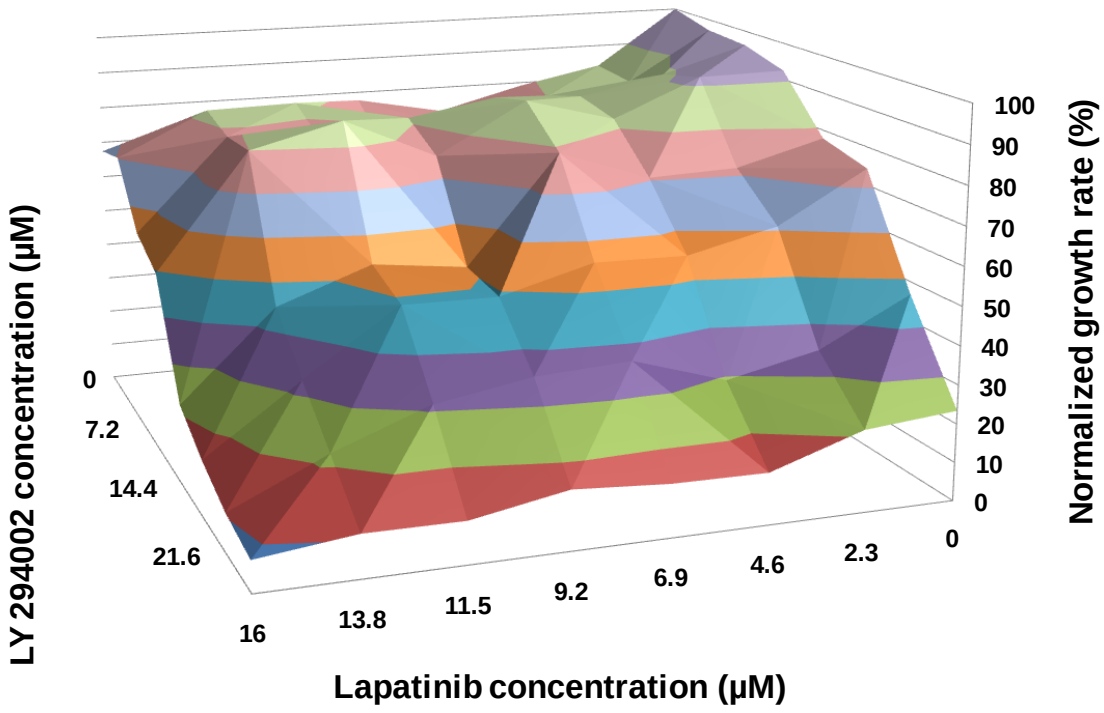

Figure 2.11. HCT116-MKI67-1000 GFP cell growth rate change by combination treatment of Lapatinib and LY 294002.

To further clarify the dose response characteristics of each drug, concentration gradients of Lapatinib and LY 294002 were plotted against each other in Figure 2.12. In both Figure 2.12(A) & (B), the weighted black lines refer to the control group (LY 294002 concentration = 0 μM as in Figure 2.12(A), and Lapatinib concentration = 0 μM as in Figure 2.12(B)). In Figure 2.12(A), the HCT116 growth rate dropped 23% in the control group, while 80% at most where LY 294002 concentration = 18 μM. The linear regression slope for control is -1.4, while for the maximum effect concentration of LY 294002 (18 μM) is -4.1. In Figure 2.12(B), the HCT116 growth rate dropped 77% in the control group, while 88% at most where Lapatinib concentration = 16 μM. The linear regression slope for control is -2.9, while for the maximum effect concentration of Lapatinib (16 μM) is -4.2. The results here suggest that Lapatinib and LY 294002 worked in agonism in the cell growth regulation of HCT116 cells.

(A)

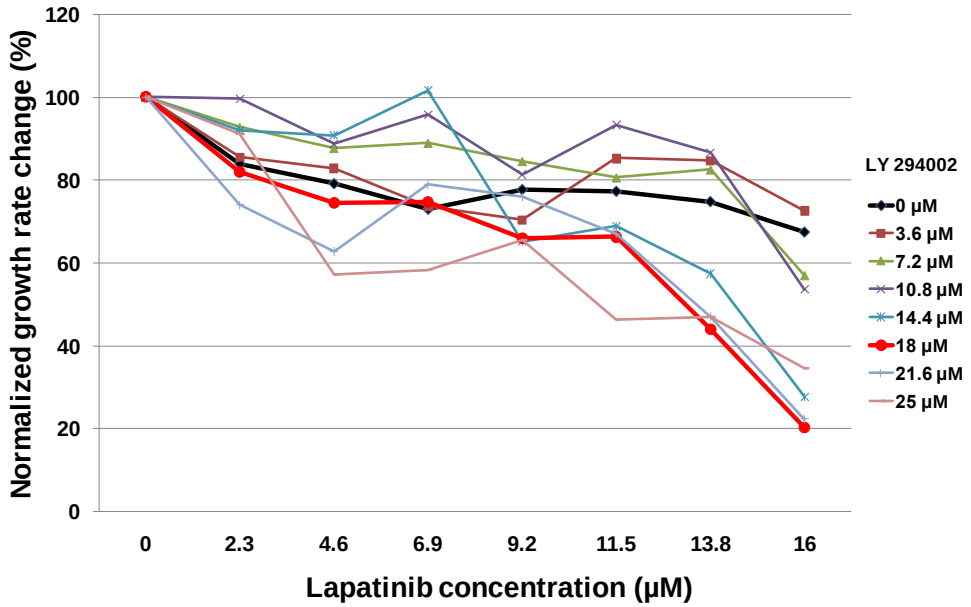

(B)

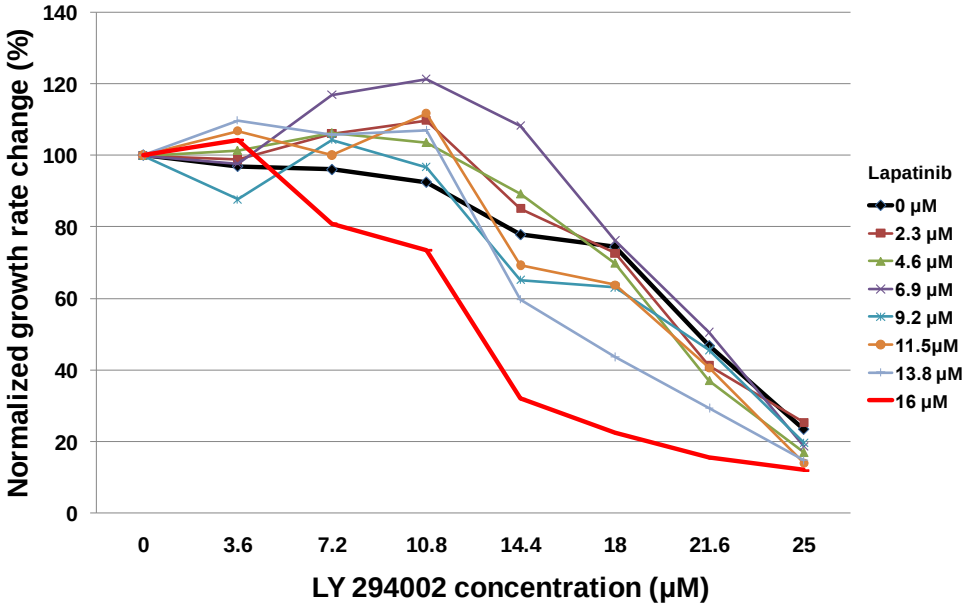

Figure 2.12. Combination effect of Lapatinib and LY 294002 in growth rate change of HCT116 cells. (A) Growth rate change by concentration gradient of LY 294002 plotted against that of Lapatinib. (B) Growth rate change by concentration gradient of Lapatinib plotted against that of LY294002.

2.6. Conclusions

Overall, we have successfully developed a fully automated high-throughput combination drug screening microfluidic live cell array with high cell seeding uniformity and utilized the platform for combinatorial gene regulation studies. This high-throughput screening system can be used to investigate combinational drug treatment effects at various concentration mixtures as well as drug dosing schemes in a sequential manner, all in high-throughput. We expect that this system can greatly improve the efficiency in finding new combination cancer therapies.

CHAPTER III

MICROFLUIDIC GEOMETRIC METERING-BASED LIVE CELL TOXIN SCREENING PLATFORM

3.1. Introduction

The microfluidic network-based gradient generator discussed in Chapter II is most widely used in high-throughput screening where generating complex gradient profiles or mixtures are needed. Such profiles and mixing ratios are determined by the microchannel network design. However, this method has many practical limitations for routine use since the generated gradient profiles or chemical mixing ratios rely on the stable flow at optimized flow rate throughout the experiment. In applications requiring multi-day drug or toxin treatments against cells, this configuration of gradient generator suffers from lack of long-term stability throughout the experiment, difficulties in repeatedly generating exactly the same profiles from run to run, consumption of large amount of reagents due to continuous flow, and subjecting cells to unwanted and potentially damaging shear stresses, which all make it challenging for routine use. Also, small variation in devices stemming from microfabrication may results in different device to device gradient profiles. Even though such changes and variations are easy to identify when characterizing devices with color dye or fluorescent dye, once these devices are used in routine, knowing the actual generated concentrations is impossible. Thus, generating reliable and repeatable concentrations and mixtures from run to run over the entire period of assay as well as from device to device becomes extremely

important. It is also difficult to implement mixing of three or more reagents with dilutions of choice unless complex microfluidic structures or dynamic control schemes are used.

The need for generating multi-reagent mixtures on-demand in a microfluidic live cell assay device can be satisfied by implementing a geometric metering approach where the mixing ratio is solely determined by the volume ratios of reagent chambers to be mixed. This microfluidic geometric metering approach was first demonstrated by Carl Hansen, *et al.*, as a robust, scalable and accurate microfluidic metering method and was termed as barrier interface metering (BIM) [25]. The geometric metering method is shown in Figure 3.1. The principle is to partition sections of the microfluidic channel at well-defined volumes and fill them separately with different solutions. These geometrically defined sections can be isolated from the microfluidic channels and mixed with other adjacent sections by actuating pneumatic control microvalves. The power and flexibility of this metering scheme was demonstrated with ultra-small volume screening of protein crystallization conditions, which is a major hurdle in structural biology efforts. However, the scheme illustrated here is limited to mixing only by adjacent chambers,

and no delivery of mixture solution was performed. In order to utilize this method in producing multi-reagent mixtures at specified mixing ratios and apply them to arrays of cell culture chambers for high-through live cell assay, robust and accurate fluid transportation method has to be also implemented.

Therefore, a novel method called pressurized membrane pumping (PMP) for robust, intact, and accurate fluid transportation in microfluidic systems was developed. Overall, we developed a geometric metering-based microfluidic concentration mixture generator capable of generating 64 mixtures of three reagents with four different concentrations for each, integrated with a 64-cell culture chamber array for combination environmental toxin screening. The cell culture chambers have arrays of single cell trapping sites to allow single cell resolution analysis of expression profile in response to the stimuli. The functionality as a microfluidic live cell environmental toxin screening platform of the developed integrated geometric metering-based mixture generator and cell culture chamber array was demonstrated.

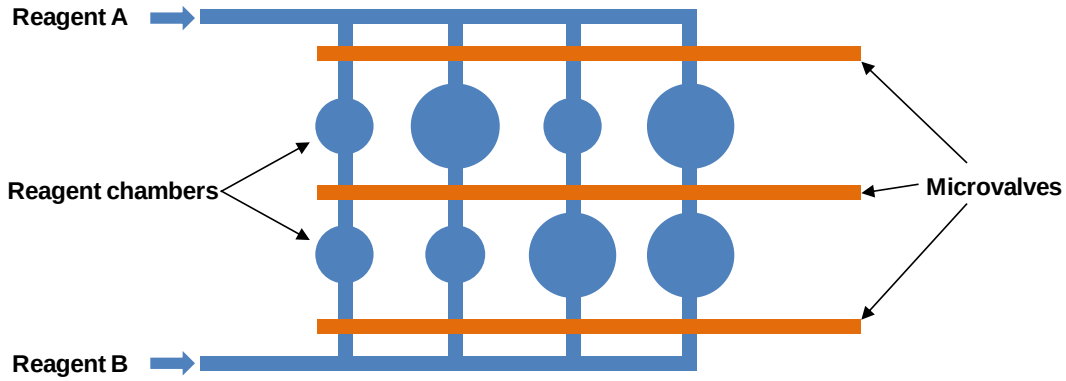

Figure 3.1. Geometric metering schematic (reproduced from [25]). Control channels are shown in orange, while fluidic channels are shown in blue. Reagents A and B can be filled separately by opening the top and bottom microvalves while closing the middle microvalve. Thereafter, reagents A and B can be mixing by diffusion when the middle microvalve is open while the top and bottom microvalves are closed.

3.2. Design and Fabrication

3.2.1. Overview

Figure 3.2(A) shows an 8-channel prototype version of the developed microfluidic geometric metering-based combination environmental toxin single cell screening platform. The device is composed of six functional components: reagent chambers; pressurized membrane pumping fluid delivery system; mixing chambers; cell culture chambers with and without single cell trapping array; cell seeding channels on the pneumatic control layer; and pneumatic valves. Of them, buffer reservoirs, reagent/mixing/cell culture chambers were all geometrically predefined.

The workflow of the developed system goes as follows. Buffer is filled into the buffer reservoirs, while reagents are filled into each reagent metering chambers. Thereafter the reagents are delivered into downstream mixing chambers by actuating the pneumatic buffer reservoir membrane valves, and allow diffusive mixing. The generated mixtures are then delivered to cell culture chambers by again actuating the buffer reservoir membrane valve.

3.2.2. Geometric Metering-based Concentration Mixture Generator

The developed geometric metering-based concentration mixture generator is capable of generating combinatorial mixtures of 3 environmental toxins each having 4 different concentrations (full capability 4^3 = 64 conditions). It can produce robust and repeatable multi-reagent mixtures on-demand at significantly reduced reagent

consumption (1/700 compared to serpentine type gradient generator over a 2-day experiment). Figure 3.2(B) shows the schematic of the principle of geometric metering-based mixture generator with fluid delivery capability for live cell assay, where two different concentrations of both reagents A and B are mixed combinatorially, generating 4 unique mixtures (2 by 2). Reagents A and B were each filled into rows of reagent chambers with two different volumes, and were subsequently driven into the downstream mixing chambers. Here the dilution and mixing ratios are "hard-wired" into the platform by specifying volume ratios between reagent chambers. In the 8-channel prototype shown in Figure 3.2(A), the three reagent channels (red, yellow, green) run perpendicular to the main flow channels and are separated from each other through pneumatically actuated microvalves. Each reagent channel has series of chambers of four different sizes (2.4, 4.8, 7.2, 9.6 nl), and all three of them are filled simultaneously using separate reagent-loaded syringes. These chambers are positioned in each reagent channel so that combinatorial mixing can be realized.

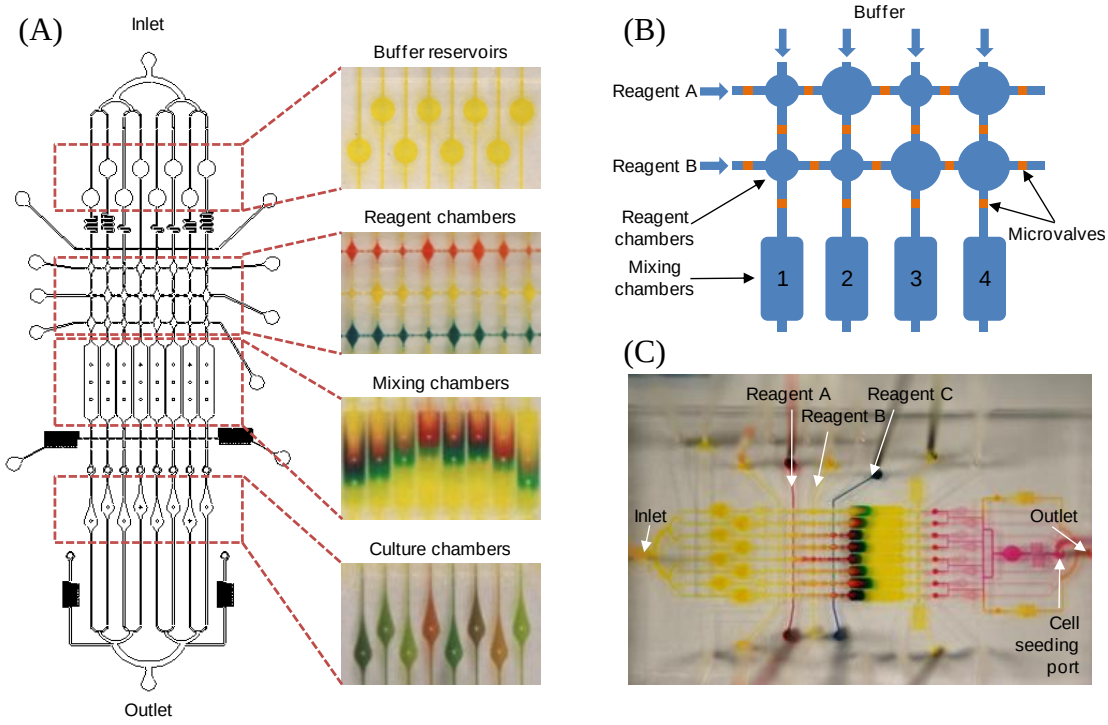

Figure 3.2. The microfluidic geometric metering-based mixture generator integrated with cell culture array. (A) The fluidic layer with magnified view of the functional regions. (B) Schematic of the principle of geometric metering-based mixture generation. Two reagents (A and B) were filled into reagent chambers at specified volumes and driven into mixing chambers for diffusive mixing, facilitating on-demand multi-reagent mixture generation. (C) Overall image of the fabricated device. Combinations of 4 different chamber sizes for reagents A (blue), B (red), and buffer (yellow) on each column generate combinatorial mixtures of 4 different dilutions of A, and B when pushed into the mixing chambers through pneumatic buffer reservoir membrane valve actuation. The pink colors indicates cell seeding path.

3.2.3. Pressurized Membrane Pumping

The so called pressurized membrane pumping (PMP) method utilizes the mechanical and structural characteristics of the PDMS multilayer microfluidic device, and introduces the pneumatic pressure as pumping power source. The PDMS microfluidic device developed for this high-throughput toxin screening consists of three layers: the thick pneumatic control layer, the fluidic membrane layer, and the glass substrate. The fluidic membrane layer is about 100 μm thick and has a channel height of 30 μm, and pneumatic pressure is introduced into the buffer reservoir membrane valve which is prefilled with DI water to prevent bubble generation during valve actuations. When positive pressure is applied to the membrane valve, at the same time the inlet valve is closed and the outlet valve is open, the membrane valve is bent down and solutions inside the buffer reservoir will be pumped out. On the contrary, when positive pressure is removed, at the same time the inlet valve is open and the outlet valve is closed, the membrane valve is open and the buffer reservoir will be refilled (Figure 3.3). The buffer reservoirs were designed with a specific volume (34 nl) to precisely deliver all three reagents into downstream mixing chambers through a single actuation of the membrane valve. The residue leftover in the buffer reservoir is negligible with this pumping method due to relative geometries of membrane thickness and channel height, as well as the pneumatic pressure applied.

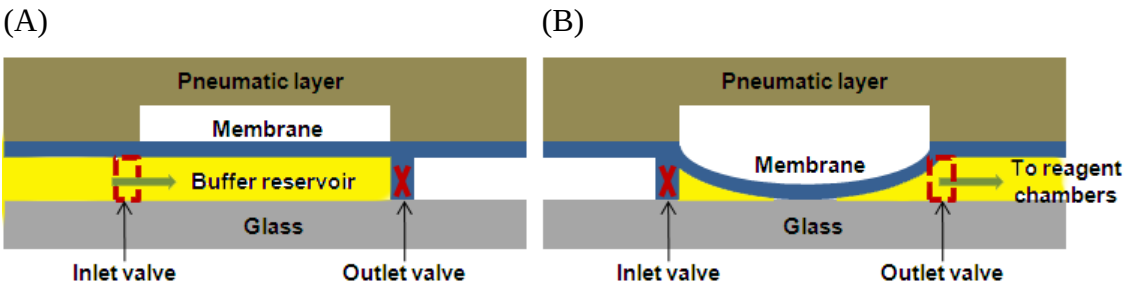

Figure 3.3. Pressurized membrane pumping. (A) Solutions driven into the buffer reservoir by actuating inlet and outlet valves. (B) Positive pressure bends down the membrane valve, solutions driven out of the buffer reservoir.

Using this scheme, there is no need to precisely time the opening and closure of the microvalves at the mixing chambers as well as the injection time for buffer syringe pump in order to completely trap reagents inside the mixing chambers.

3.2.4. Diffusive Mixing and Cell Seeding

Diffusive mixing of reagents inside the mixing chambers was employed, since reagent mixtures typically needed to be generated only every 4 hours throughout the multi-day experiment. Supporting pillars were added to the mixing chambers to prevent chamber collapse during device bonding. Cell culture chambers are located downstream of these mixing chambers, and the overall channel height is 30 μm. Cell culture chambers were designed both with single cell traps and without. In each cell culture chamber with single cell traps, more than 200 hydrodynamic trapping structures were designed into an asymmetric array with lateral displacements between neighboring rows to maximize the trapping efficiency (Figure 3.4(A)). The cell traps are hanging from the channel top so that the traps are elevated from the channel bottom with a 3 μm gap. For both kinds of cell culture chambers, each chamber has cell seeding via holes connected to a single cell seeding port on the pneumatic layer so that cells can be loaded directly into the cell culture chambers simultaneously (Figure 3.4(B)). Two side-channels with high fluidic resistance were implemented near the cell seeding channels to overcome the sidewall effect, ensuring uniform cell seeding into all eight culture chambers. The overall image of the fabricated device is shown in Figure 3.2(C).

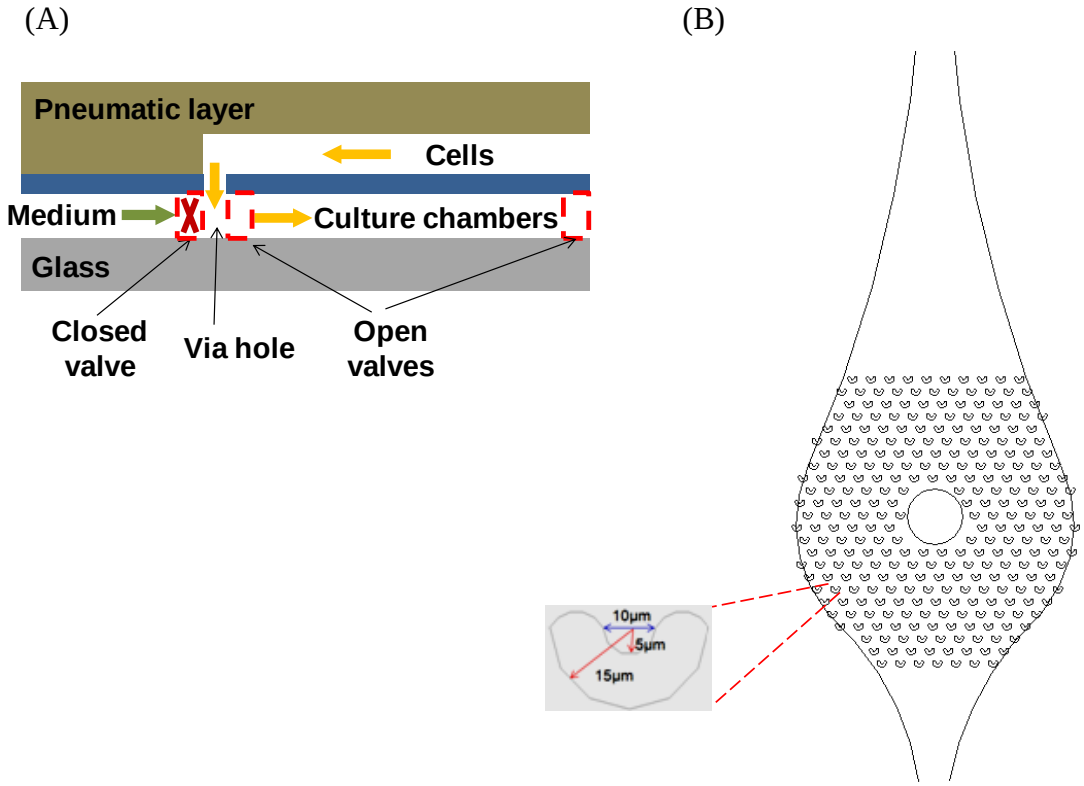

Figure 3.4. Single cell seeding and trapping. (A) Schematic of the cell seeding. (B) Asymmetric single cell trapping array with lateral displacement between neighboring rows inside one cell culture chamber. The enlarged inset shows the geometry of a single cell trap.

3.2.5. Device Fabrication

The device was fabricated with poly(dimethylsiloxane) (PDMS, Sylgard 184, Dow Corning), and coated with fibronectin for enhanced cell attachment before cell loading. The pneumatic control layer is fabricated by cast molding a thick layer of PDMS, and the fluidic membrane layer is fabricated by spin coating PDMS at 700 rpm for 40 s. Thereafter the two layers were bonded with oxygen plasma treatment and via holes were made by stainless steel punches. The assembled PDMS block was finally bonded to glass substrate using oxygen plasma treatment.

3.3. Experimental

The functionality of the geometric metering-based mixture generator was first characterized with color dyes. For the opening and closure of general pneumatic valves, 7 psi positive pressure and -2 psi negative pressure were used. While for the buffer reservoir membrane valve, 3 psi positive pressure was used for pumping out buffer solution for reduced flow rate and improved controllability and robustness. The run to run and device to device repeatability of the developed geometric metering-based microfluidic multi-reagent mixer and the network-based gradient generator was characterized with fluorescein isothiocyanate (FITC) and rhodamine B isothiocyanate (RBITC) in comparison. The network-based gradient generator used here consists of a dual-inlet gradient generator and corresponding eight downstream chambers (Figure 2.1). FITC and DI water were injected at the same flow rate (1 μl/min) via two inlets,

and the repeatability was characterized by measuring the fluorescence intensity in eight branching chambers after a 5-minute period for the flow to stabilize. The geometric metering-based mixer used here is a simplified version of Figure 3.2(C) which removes the cell seeding section. RBITC was filled into reagent chambers with a syringe pump, and driven into mixing chambers subsequently. The diffusive mixing took place after within 4 h period in the 37°C incubator, and the mixing process was characterized at near inlet, middle, near outlet locations of each mixing chamber by measuring fluorescence intensities.

After characterization of the developed platform, the effect of potent atmospheric pollutants polyaromatic hydrocarbon (PAH) pyrene on regulating gene expression in rat hepatoma (H4IIE) cells with eGFP reporter was studied on the cell population level. Though only pyrene treatment was demonstrated, the device is fully capable of PAH mixture treatment as shown in the previous geometric metering-based mixture generator section. H4IIE cells were seeded via the cell seeding port on the pneumatic layer (Figure 3.2(C)), flowing into the fluidic layer via through holes, and trapped inside the cell culture chambers. After the cells attached to the substrate, different concentrations of pyrene solutions were applied to each cell culture chamber every 4 h, for a total treatment time of 24 h. All operations were automatically controlled by a Labview® interface, enabling fully automated 2-day screening experiment. Fluorescence images were acquired with a Zeiss 200M inverted microscope using an AxioCam MRM Rev 2 camera (Carl Zeiss) and analyzed with ImageJ (NIH) by measuring the sum of fluorescence intensity per cell area.

Single cell trapping and culture have been first tested with a simplified one channel cell seeding and culture scheme (Figure 3.5(A)), and then performed with the developed geometric metering-based live cell assay platform where the cell seeding port and micropillar filter were placed on the pneumatic layer. The micropillar filter was implemented to exclude extra cellular matrix materials and conjugated multiple cells. Microvalves can isolate the single cell array from cell seeding and medium supply ports, efficiently eliminating floating cell migration from cell seeding channel and micropillar filter, as well as continuous perfusion of medium caused by pressure residue after stopping medium injection. Supporting pillars were introduced to cell culture chambers to maintain the 3 μm gap between channel bottom and single cell traps. The cell handling procedures were the same as the population-based cell seeding and culture. Cell culture was performed in two ways. In one method, the microfluidic device was tilted at 20° to maintain cell position inside a 37°C, 5% CO_2 incubator for cell attachment. In another approach, perfusion of culture medium was applied after seeding to keep cells with hydrodynamic pressure. With the perfusion method, the seeded H4IIE cells were cultured inside a Zeiss Axiovert 200M microscope incubator (Carl Zeiss).

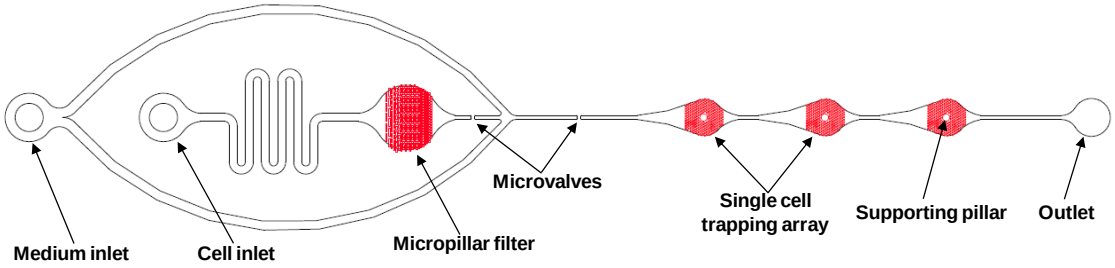

Figure 3.5. Single cell trapping and culture device.

3.4. Results and Discussion

3.4.1. Functionality Validation

Figure 3.6 shows the operation procedures of the developed geometric metering concentration mixture generator device. From left to right, buffer injection, reagent injection, reagent delivery by pressurized membrane pumping into mixing chambers, diffusive mixing, mixture delivery into cell culture chambers, and mixture regeneration were all successfully demonstrated with color dyes.

Diffusive mixing was slow in the mixing chambers due to extended chamber length (4.5 mm). However, the increased ambient temperature in the cell culture incubator (37°C) allowed complete mixing to take place within a 4 h period, which is enough for periodic medium or toxin replenishment in the cell culture chambers (Figure 3.7).

One issue with the above experiments was that the solutions in different channels were delivered at different paces with the pressurized membrane pumping. This is because of the unequalized fluidic resistances in different channels, and can be solved by introducing compensating serpentine timing channels between buffer reservoirs and reagent chambers (Figure 3.8). With the timing channels, not only the fluid delivery uniformity was improved, but also robustness of the pressurized membrane pumping method was enhanced.

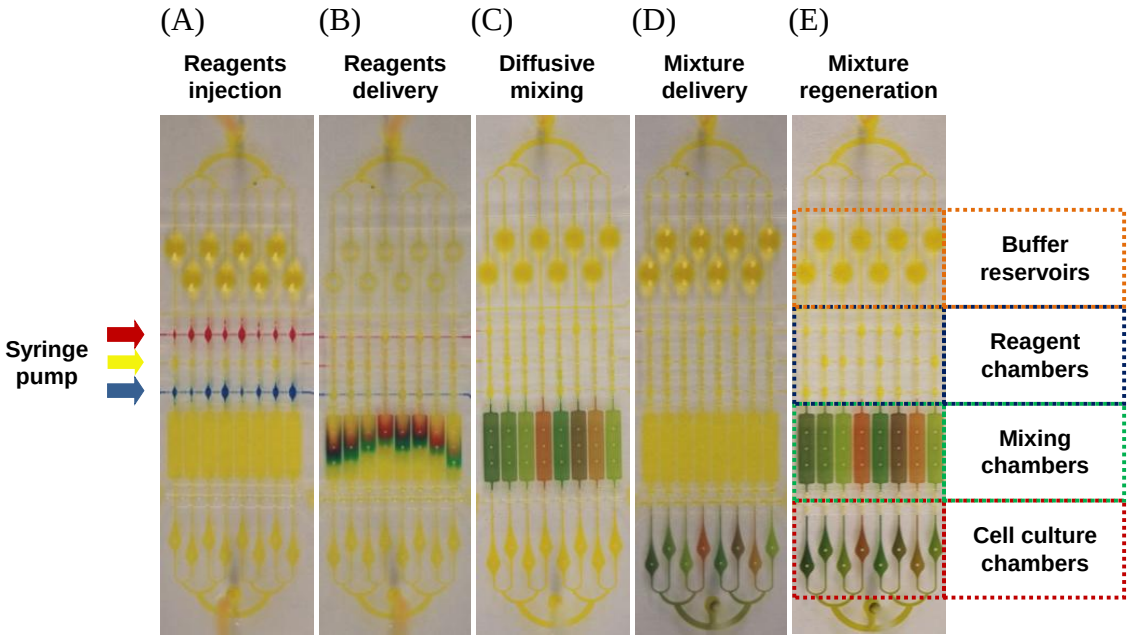

Figure 3.6. Working procedures of the geometric metering-based mixture generator. (A) Pre-filling the whole device with buffer first (yellow), followed by reagent loading into the corresponding chambers (red, yellow, blue). (B) Driving reagents into the mixing chambers by pressurized membrane pumping. (C) Diffusive mixing of the reagents. (D) Delivering generated mixtures into each cell culture chamber. (E) Regeneration of reagent mixtures.

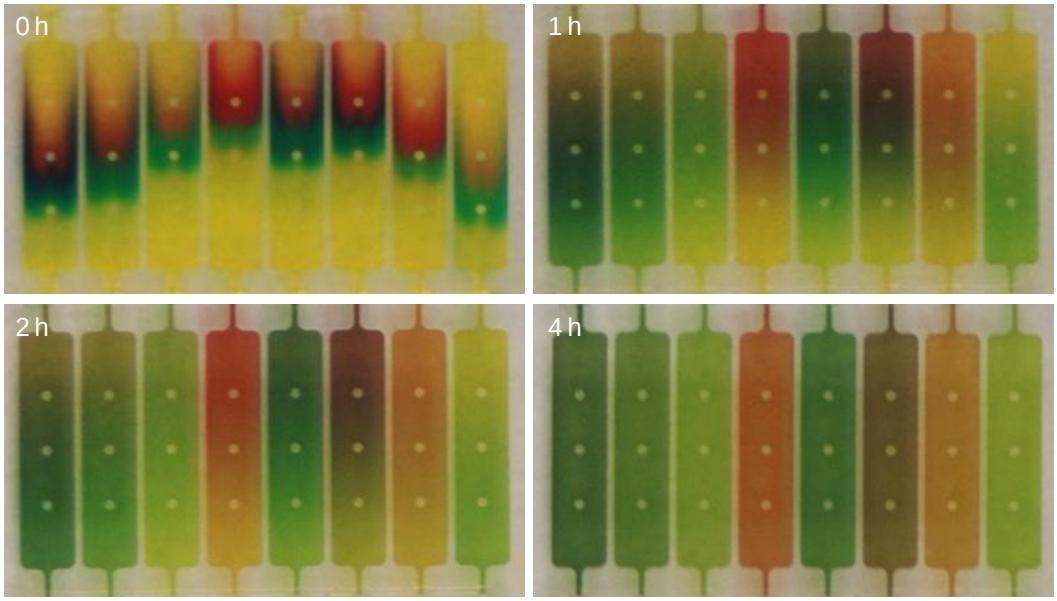

Figure 3.7. Timelapse images showing the diffusive mixing process in the 37°C incubator.

(A) w/o timing channels (B) w/ timing channels

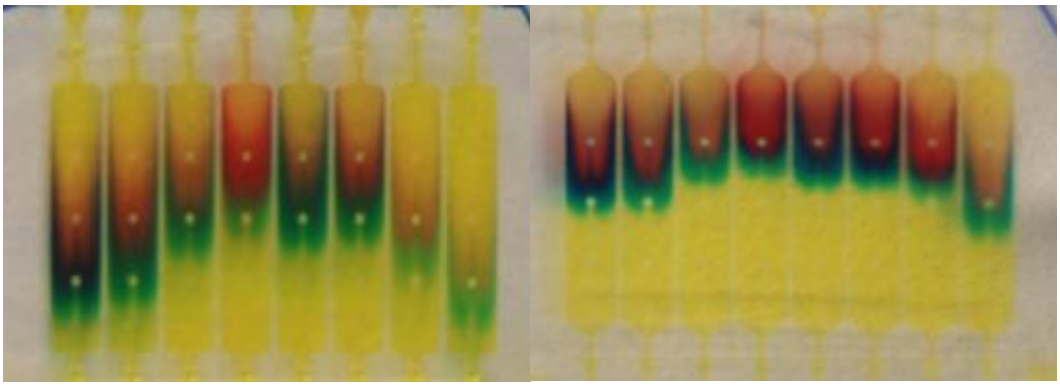

Figure 3.8. Comparison of the uniformity of reagents delivery into mixing chambers by pneumatically actuating the buffer reservoirs microvalves. (A) Non-uniform reagent delivery in the absence of timing channels. (B) Uniform reagent delivery when using timing channels.

3.4.2. Repeatability Comparison

The run to run and device to device repeatability was compared with FITC and RBITC between microfluidic network-based gradient generator and the geometric metering-based concentration mixture generator (Figures 3.9 & 3.10). Figure 3.9 shows the run-to-run normalized fluorescence intensity profiles among different channels in the network-based gradient generator and geometric metering-based mixture generator with 3 repeats each. Figure 3.10 shows the device-to-device normalized fluorescence intensity profiles in the network-based gradient generators and geometric metering-based mixture generators with 3 repeats each. From run-to-run, the geometric metering-based mixture generator showed obvious improvement in repeatability with 10% coefficient of variance (C.V.) compared to C.V. = 22% of the network-based gradient generator. From device-to-device, the geometric metering-based mixture generator again showed significant improvement in repeatability with C.V. = 6% compared to C.V. = 20% of the network-based gradient generator. This significant improvement of repeatability stems from the static mixture generation and fluid delivery nature of geometric metering-based mixture generator compared to the dynamic continuous flow mixing characteristic of the conventional network-based gradient generator.

(A) (B)

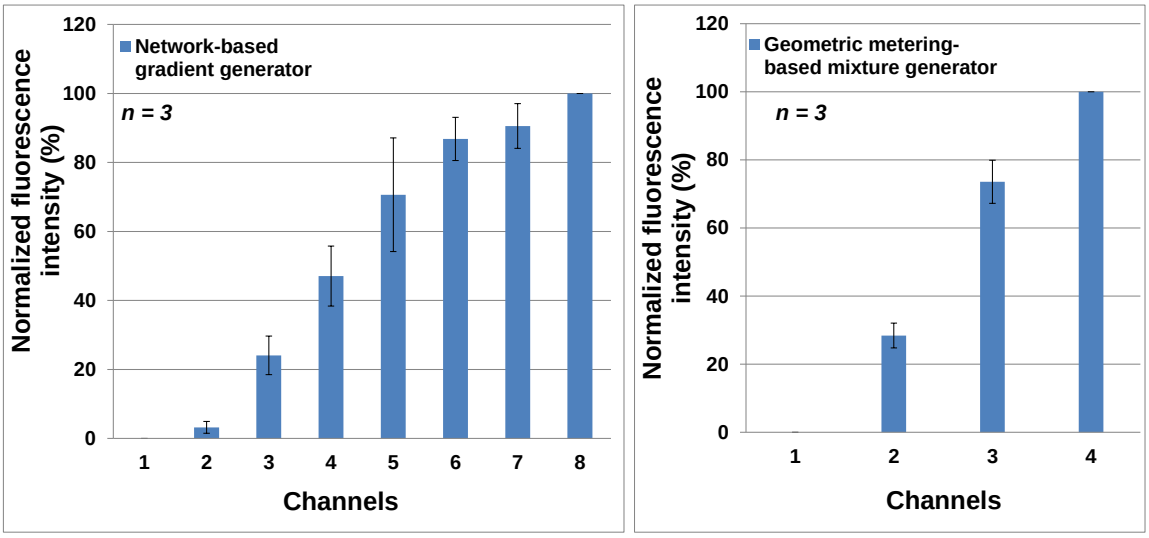

Figure 3.9. Run-to-run comparison of the repeatability of the network-based gradient generator and the geometric metering-based mixture generator. (A) Normalized fluorescence intensity profile in the network-based gradient generator with 3 repeats, showing large standard deviation. (B) Normalized fluorescence intensity profile of different channels having different reagent chambers of the geometric metering-based mixture generator with 3 repeats, showing the small standard deviation.

(A) (B)

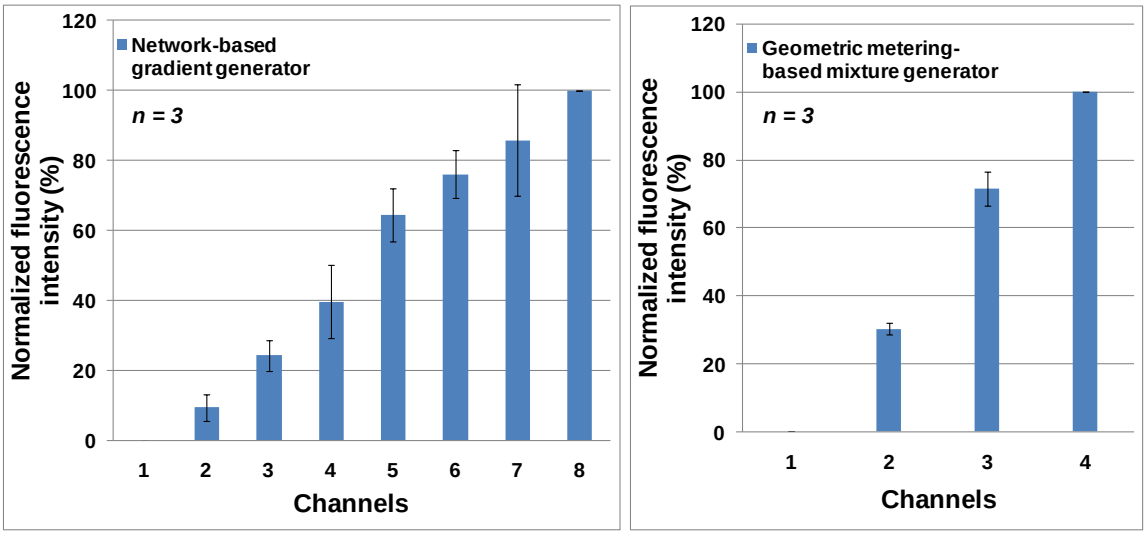

Figure 3.10. Device-to-device comparison of the repeatability of the network-based gradient generator and the geometric metering-based mixture generator. (A) Normalized fluorescence intensity profile in the network-based gradient generators (n = 3), showing large standard deviation. (B) Normalized fluorescence intensity profile of different channels having different reagent chambers of the geometric metering-based mixture generators (n = 3), showing the small standard deviation.

3.4.3. Environmental Toxin Screening

Polyaromatic hydrocarbons (PAHs) are potent atmospheric pollutants, which are carcinogenic, mutagenic, and teratogenic. PAHs are typically generated by incomplete combustion, and can also come from cooking meat at high temperatures. PAHs exhibit concentration-dependent toxicity effect to human and animal cells, and the toxicities of individual molecules have been studied intensively. However, PAHs typically come in the form of mixtures of isomers, causing great difficulties in understanding and determining the concentration-dependent mixture interactions. This kind of study requires high-throughput and robust screening against a large range of concentration mixtures of multi-reagents, which is difficult to be achieved by the conventional network-based gradient generators. Our developed geometric metering-based mixture generator can be utilized for such systematic investigations of the interaction patterns of PAHs mixtures in a high-throughput fashion.

As the functionality and repeatability performance were characterized with color dyes and fluorescent dyes, we implemented this method into environmental toxin screening of rat hepatoma (H4IIE) cells. The comparison of repeated experiment results

between three different live cell screening methods further validated the utility of this developed geometric metering-based concentration mixture generator device. Environmental toxin pyrene was applied to GFP tagged H4IIE cells cultured in the 24-well plate, microfluidic network-based gradient generator device, and the developed geometric metering-based mixture generator device at different concentrations, respectively, with three repeats each. Figure 3.11 clearly shows that the C.V. of the geometric metering-based device (5%) was much closer to that of standard 24-well plate results (3%), while the C.V. of network-based device was much larger (12%). However, one drawback of the geometric metering-based device is the lack of control (concentration = 0), therefore in Figure 3.11(A) & (B), the normalized fluorescence intensity change for pyrene concentration = 1.25 μM was adjusted for the convenience of comparison between standard deviations.

(A) (B)

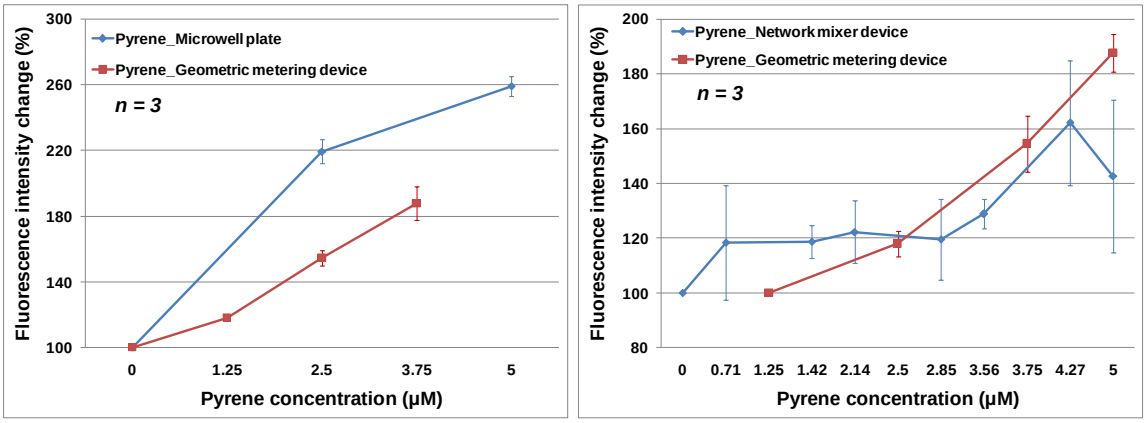

Figure 3.11. Comparison of the repeatability with pyrene treatment of H4IIE cells between the network-based gradient generator, the geometric metering-based mixture generator, and the microtiter plate. (A) Comparison of the repeatability of pyrene treatment between the microtiter plate and the geometric metering-based mixture generator (n = 3). (B) Comparison of the repeatability of pyrene treatment between the network-based gradient generator and the geometric metering-based mixture generator (n = 3). The normalized fluorescence intensity of pyrene concentration = 1.25 μM was adjusted for the convenience of comparison between standard deviations.

3.4.4. Single Cell Trapping and Culture

The developed asymmetric hydrodynamic single cell trapping array with lateral displacements between neighboring rows significantly improved the trapping efficiency. The optimized trap geometry as well as the reduced channel height improved the selectivity of single cells over two or multiple cells to be trapped. This optimized design resulted in single cell seeding efficiency of 80%, with the remaining 10% of traps having two cells and 5% having multiple cells, and with 5% vacancy (Figure 3.12(A)). The cell attachment and culture by tilting the microfluidic device at 10° inside a 37°C, 5% CO_2 incubator was shown in Figure 3.12(B). In the perfusion method, the seeded H4IIE cells were cultured inside a Zeiss Axiovert 200M microscope incubator (Carl Zeiss). Cell attachment, growth, and part of dividing were observed by timelapse imaging (Figure 3.12(C)).

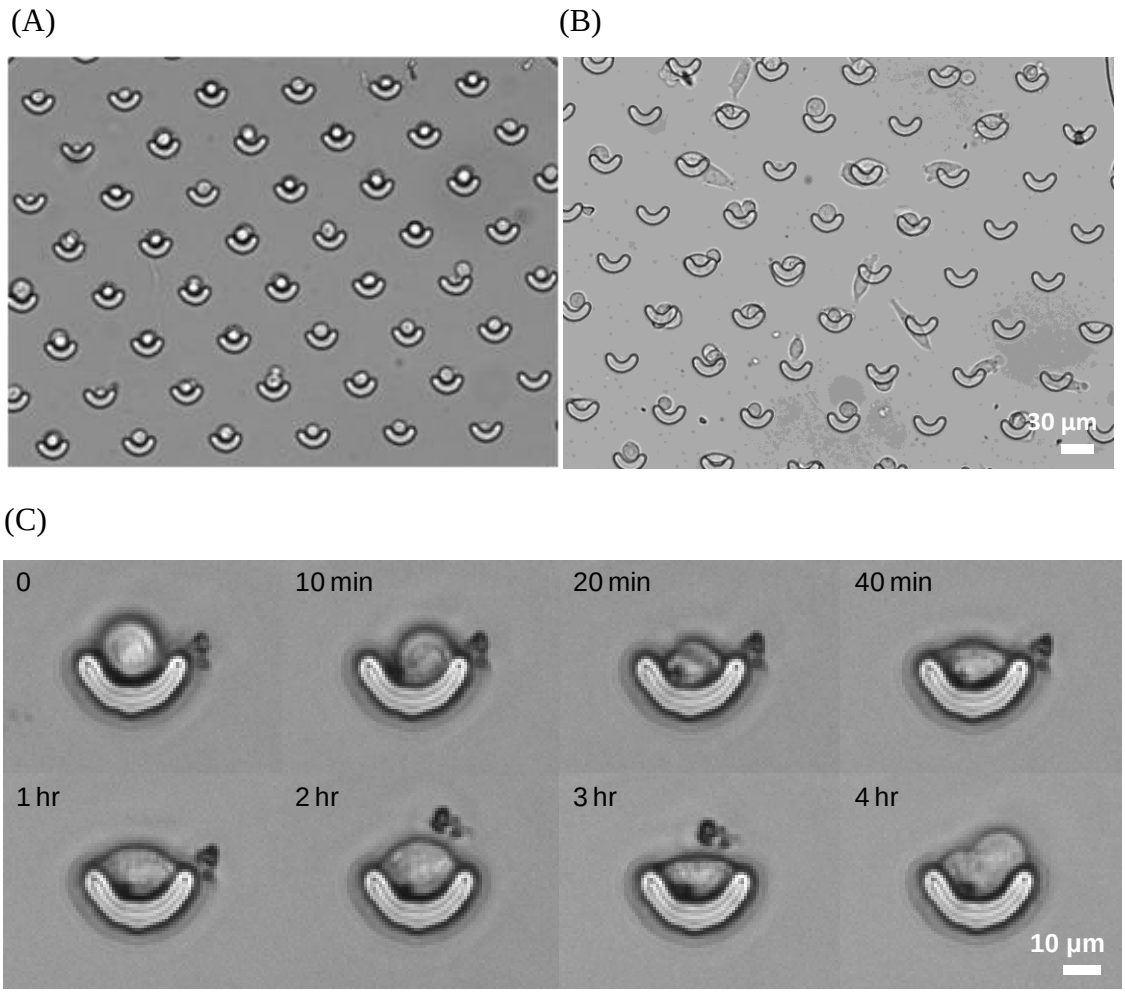

Figure 3.12. Hydrodynamic single cell trapping and culture. (A) Single cell seeding result with the developed hydrodynamic trapping scheme. (B) Cell attachment after 3 h of incubation tilted at 10°. (C) Timelapse images showing a single cell trapping, attaching, growing, and dividing with perfusion flow in a Zeiss Axiovert 200M microscope incubator.

CHAPTER IV

CONCLUSION AND FUTURE WORK

4.1. Conclusion

In this thesis, robust and high-throughput microfluidic mixture generation devices were developed and utilized for combination live cell screening versus drugs and toxins.

A microfluidic network-based gradient generator capable of producing pair-wised gradient profile of two drugs was integrated with a 8 by 8 cell culture array for the study of synergistic effect of cancer drug Lapatinib and kinase inhibitor LY 294002 on humane colorectal cancer cell HCT116 tagged with MKI67-GFP promoter-reporter group. Symmetric cell seeding channels improved the uniformity of cell seeding. Both GFP reporter activity and cell growth rate were recorded and used as the measures to evaluate the drug effects, and strong correlation between these two methods was observed. Synergy was reported with sequential treatment of the two drugs by measuring cell growth rate change.

However, due to the limitations of this network-based mixer in large reagent consumption, continuous stable flow requirement, and subjecting cells to shear stresses, a novel microfluidic mixer which implemented the geometric metering approach was developed. This geometric metering method is inherently little reagent consumption, robust and scalable since the mixing ratio is solely dependent on the volumes of reagent chambers. A novel and straightforward microfluidic fluid delivery method called

pressurized membrane pumping (PMP) was developed and integrated with the geometric metering method to build a fully functional robust and high-throughput microfluidic cell culture and toxin screening platform. Though only a prototype 8-channel device was demonstrated for functionality, this scheme can be readily transformed into large scale screening platform due to the intrinsic scalability of geometric metering method. This device showed improved repeatability over conventional network-based gradient generator. The effect of potent atmospheric pollutants polyaromatic hydrocarbon (PAH) mixtures (Pyrene, Benzo(a)Pyrene, and 20-Methylcholanthrene (20-MCA)) on regulating gene expression in rat hepatoma cells (H4IIE) with eGFP reporter was studied.

4.2. Future Work

Single cell assay not only pushes the resolution to an individual cell level, but also offers enormous potentials in studying cell heterogeneity and sub-cellular processes. Single cell trapping enables easy tracking/analysis of single cell level gene expression, which provides quantitative information on the heterogeneous behaviors of individual cells not obtainable through population-based studies. Hydrodynamic trapping of individual cells with physical obstacles offers a simple, effective, and physiologically favorable solution for separating single cells.

The developed single cell trapping and culture method will be integrated with the developed geometric metering-based microfluidic live cell screening platform to quantitatively measure the heterogeneity of cell behaviors in response to combination

toxin treatment, and provide the first-hand data for studying gene expression regulation at the single cell level in a high-throughput fashion. We believe this advancement will offer the flexibility of cell microenvironment control by varying environmental stimuli, while maintaining high-throughput capability.

REFERENCES

1. G. R. Zimmermann, , J. Leh ár, and C. T. Keith, *Drug Discovery Today*, 2007, **12**, 34-42.
2. E. Frei III, M. Karon, R. H. Levin, E. J. Freireich, R. J. Taylor, *et al.*, *Blood*, 1965, **26**, 642-656.
3. L. D. Mayer, and A. S. Janoff, *Mol Interv.*, 2007, **7**, 216-23.
4. M. L. Toews, and D. B. Bylund, *Proceedings of the American Thoracic Society*, 2005, 282-289.
5. M. L. Yarmush, and K. R. King, *Annu. Rev. Biomed. Eng.*, 2009, **11**, 235-257.
6. I. Meyvantsson, and D. J. Beebe, *Annu. Rev. Anal. Chem.*, 2008, **1**, 423-449.
7. S. Takayama, E. Ostuni, P. LeDuc, K. Naruse, D. E. Ingber, *et al.*, *Nature*, 2001, **411**, 1016-1016.
8. F. K. Balagadd é, L. You, C. L. Hansen, F. H. Arnold, and S. R. Quake, *Science*, 2005, **309**, 137-140.
9. P. J. Hung, P. J. Lee, P. Sabounchi, R. Lin, and L. P. Lee, *Biotechnol Bioeng.*, 2005, **89**, 1-8.
10. A. I. Rodr íguez-Villarreal, M. Arundell, M. Carmona, and J. Samitier, *Lab Chip*, 2010, **10**, 211-219.
11. Y. Xia, and G. M. Whitesides, *Annu. Rev. Mater. Sci.*, 1998, **28**, 153-184.
12. S. A. Sundberg, *Curr. Opin. Biotechnol.*, 2000, **11**, 47-53.
13. Z. Wang, M. C. Kim, M. Marquez, and T. Thorsen, *Lab Chip*, 2007, **7**, 740-745.

14. P. J. Lee, P. J. Hung, V. M. Rao, and L. P. Lee, *Biotechnol. Bioeng.*, 2006, **94**, 5-14.

15. A. Schmid, H. Kortmann, P. S Dittrich, and L. M. Blank, *Curr. Opin. Biotechnol.*, 2010, **21**, 12-20.

16. A. Adamo, and K.F. Jensen, *Lab Chip*, 2008, **8**, 1258-1261.

17. B. Huang, H. Wu, D. Bhaya, A. Grossman, S. Granier, B. K. Kobilka, and R. N. Zare, *Science*, 2007, **315**, 81-84.

18. H. Kortmann, F. Kurth, L. M. Blank, P. S. Dittrich, and A. Schmid, *Lab Chip*, 2009, **9**, 3047-3049.

19. J. Nilsson, M. Evander, B. Hammarström, and T. Laurell, *Anal Chim Acta.*, 2009, **649**, 141-57.

20. D. D. Carlo, L. Y. Wu, and L. P. Lee, *Lab Chip*, 2006, **6**, 1445-1449.

21. T. M. Keenan, and A. Folch, *Lab Chip*, 2008, **8**, 34-57.

22. N. L. Jeon, S. K. W. Dertinger, D. T. Chiu, I. S. Choi, A. D. Stroock, and G. M. Whitesides, *Langmuir*, 2000, **16**, 8311-8316.

23. S. K. W. Dertinger, D. T. Chiu, N. L. Jeon, and G. M. Whitesides, *Anal. Chem.*, 2001, **73**, 1240-1246.

24. J. Kim, D. T., M. Hegde, K. Rege, and A. Jayaraman. *Thirteenth International Conference on Miniaturized Systems for Chemistry and Life Sciences*, 2009, 1494-1496.

25. C. L. Hansen, E. Skordalakes, J. M. Berger, and S. Q. Quake, *Proceedings of the National Academy of Sciences*, 2002, 16531-16536.

APPENDIX A

MASK DESIGN: ALIGNMENT MARK

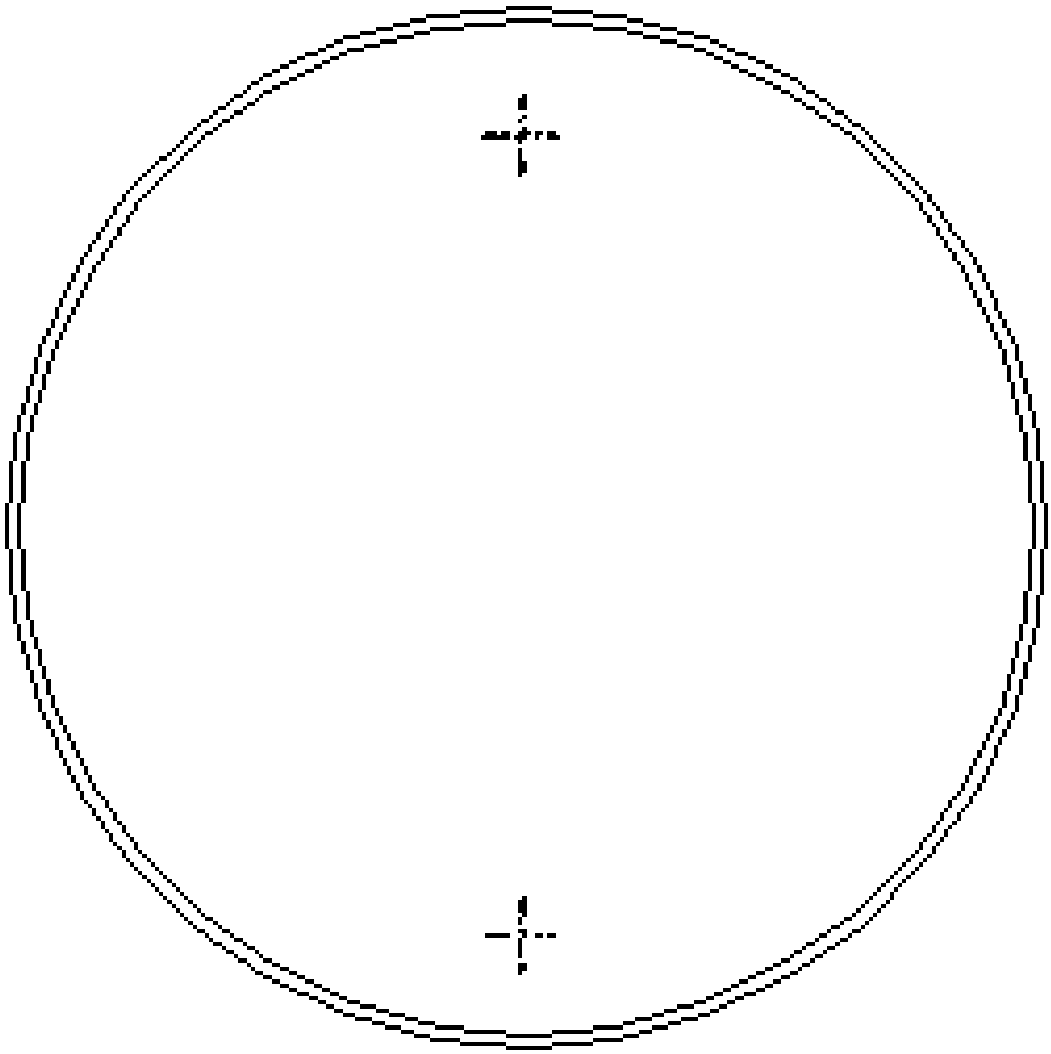

Figure A.1. Mask layout of the alignment mark (alignment mark.dwg)**.**

MASK DESIGN: FLUIDIC LAYER WITHOUT SINGLE CELL ARRAY

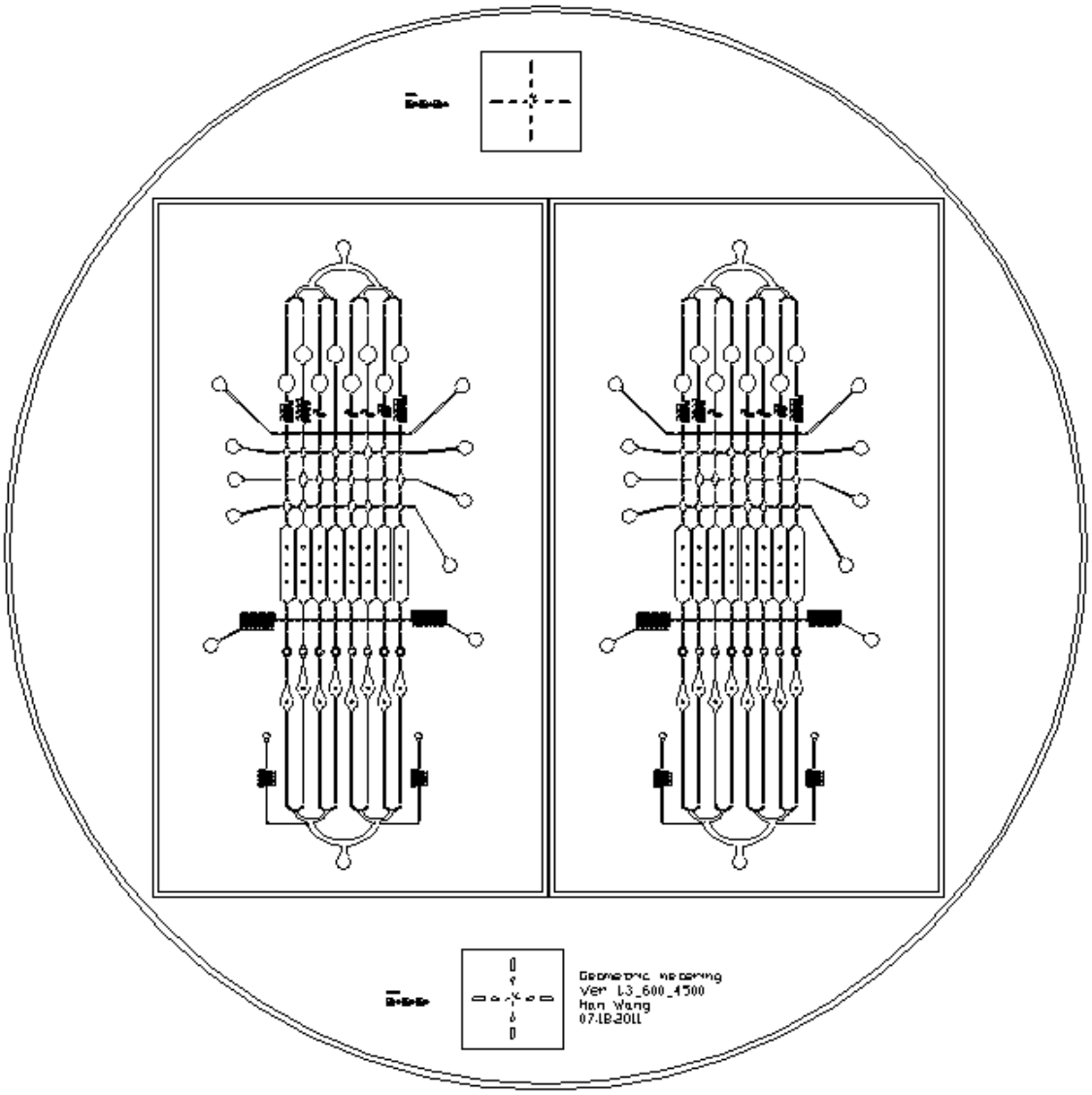

Figure A.2. Mask layout of the fluidic layer without single cell array (fluidic layer without single cell array.dwg)**.**

MASK DESIGN: FLUIDIC LAYER WITH SINGLE CELL ARRAY

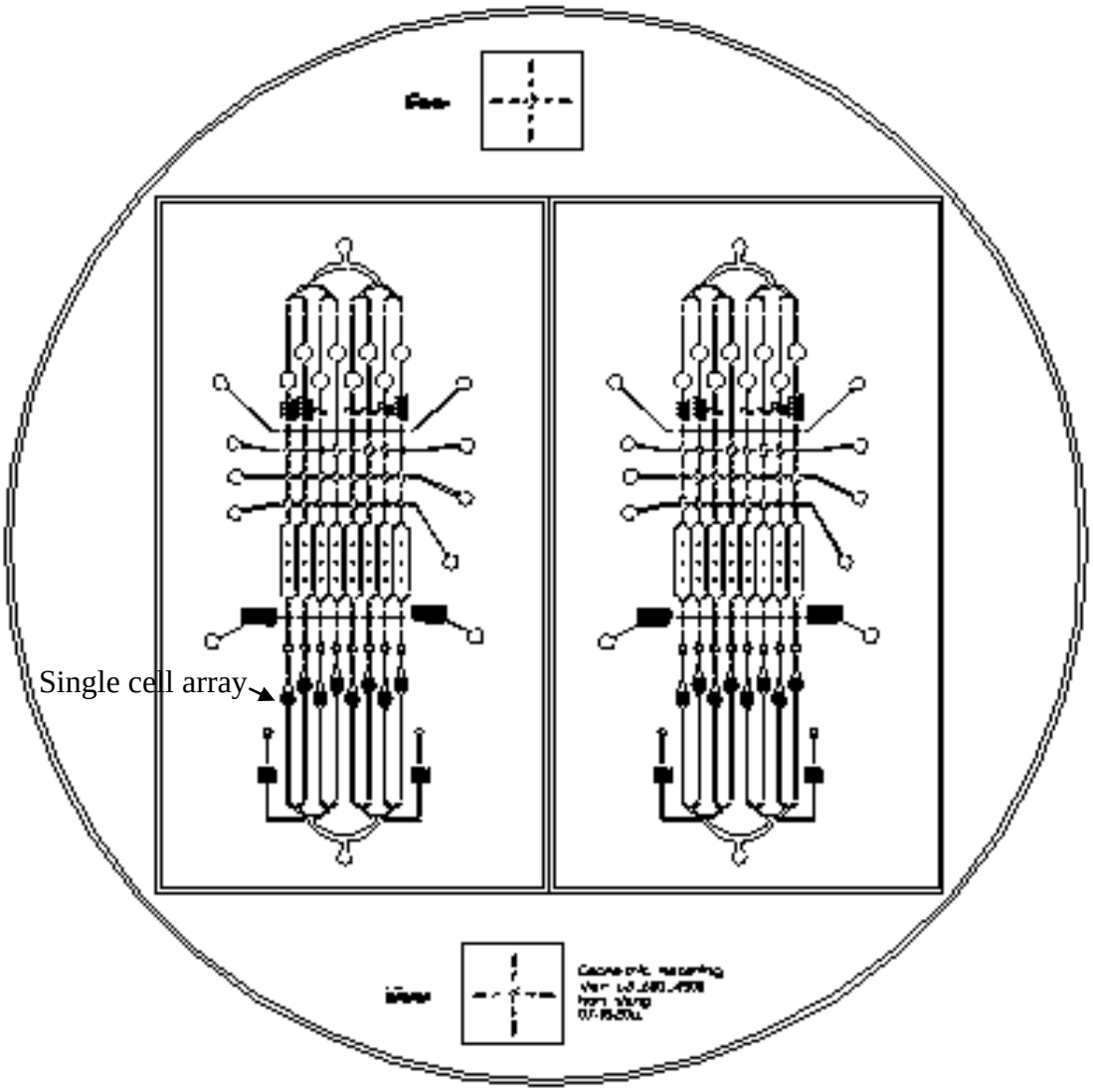

Figure A.3. Mask layout of the fluidic layer with single cell array (fluidic layer with single cell array.dwg)**.**

MASK DESIGN: PNEUMATIC LAYER

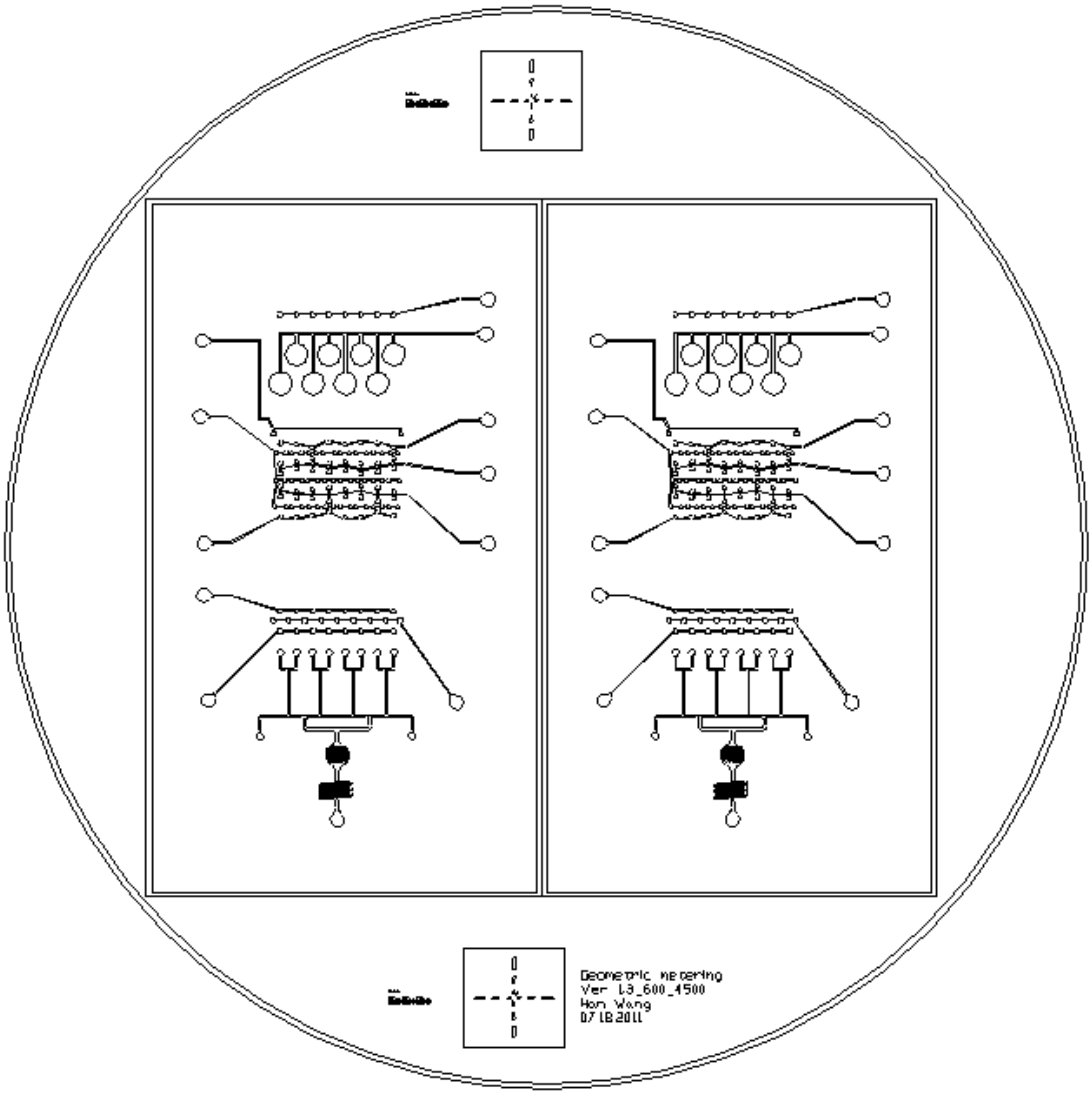

Figure A.4. Mask layout of the pneumatic layer (pneumatic layer.dwg)**.**

APPENDIX B

MASTER FABRICATION PROCEDURE

B.1. Aluminum Alignment Mark Patterning Procedure

1. Clean the 3 inch silicon wafer with acetone, IPA, and DI water in sequence and dry with N_2 gas

2. Dehydrate baking at 200 ℃ for 10 minutes

3. Deposit Al layer using an E-beam evaporator to a thickness of 2000 Å

4. Repeat steps 1 and 2

5. Spin coat Microposit S1818 photoresist (Rohm and Haas Electronic Material LLC, Marlborough, MA) on the silicon wafer at 4000 rpm for 30 seconds with an acceleration time of 5 seconds

6. Soft baking at 95 ℃ for 10 minutes, cool down

7. Expose UV using a mask aligner (MJB3, SUSS MicroTec Inc., Waterbury Center, VT) at 12 mW/cm^2 (wavelength: 320 nm) for 14 second with a photomask having alignment marks

8. Develop the pattern using MF-319 developer (Rohm and Haas Electronic Material LLC, Marlborough, MA) for 20-40 seconds

9. Rinse in DI water and dry with N_2 gas. Only the alignment marks were covered with photoresist

10. Etch uncovered Aluminum with Aluminum etchant for about 20 min

11. Rinse the wafer with acetone, IPA, and DI water in sequence, and dry with N_2 gas

B.2. Fluidic Layer with Single Cell Trapping Array Master Fabrication Procedure

1. Rinse the alignment mark patterned silicon wafer with acetone, IPA, and DI water in sequence, and dry with N_2 gas

2. Dehydrate baking at 200 ℃ for 10 minutes

3. Spin coat 3 μm thick photoresist (SU-8™ 2002, Microchem, Inc., Newton, MA) on the alignment mark pattered silicon wafer at 750 rpm for 40 seconds

4. Soft baking at 95 ℃ hotplate for 5 minutes, cool down

5. Expose UV using a mask aligner (MA6, SUSS MicroTec Inc., Waterbury Center, VT) at 120 mJ/cm^2 with the fluidic layer photomask which has single cell array

6. Post exposure baking at 95 ℃ for 6 minutes, cool down

7. Develop the patterns using Microposit Thinner Type P (Shipley Co., Marlborough, MA) for about 30 seconds

8. Rinse with IPA and DI water, and dry with N_2 gas

9. Spin coat 27 μm thick photoresist (SU-8™ 2025, Microchem, Inc., Newton, MA) on the pre- pattered silicon wafer at 3500 rpm for 40 seconds

10. Soft baking at 65 ℃ for 5 minutes, followed by 95 ℃ baking for 10 minutes, cool down

11. Expose UV using a mask aligner (MA6, SUSS MicroTec Inc., Waterbury Center, VT) at 180 mJ/cm^2 with the fluidic layer photomask

12. Post exposure baking at 65 ℃ for 3 minutes, followed by 95 ℃ baking for 10 minutes, cool down

13. Develop the patterns using Microposit Thinner Type P (Shipley Co., Marlborough, MA) for about 3 minutes

14. Rinse with IPA and DI water, and dry with N_2 gas

B.3. Fluidic Layer without Single Cell Trapping Array Master Fabrication Procedure

1. Rinse a bare 3 inch silicon wafer with acetone, IPA, and DI water in sequence, and dry with N_2 gas

2. Dehydrate baking at 200 ℃ for 10 minutes

3. Spin coat 30 μm thick photoresist (SU-8™ 2025, Microchem, Inc., Newton, MA) on the pre- pattered silicon wafer at 3000 rpm for 40 seconds

4. Soft baking at 65 ℃ for 5 minutes, followed by 95 ℃ baking for 10 minutes, cool down

5. Expose UV using a mask aligner (MA6, SUSS MicroTec Inc., Waterbury Center, VT) at 200 mJ/cm^2 with the fluidic layer photomask which doesn't have single cell array

6. Post exposure baking at 65 ℃ for 3 minutes, followed by 95 ℃ baking for 10 minutes, cool down

7. Develop the patterns using Microposit Thinner Type P (Shipley Co., Marlborough, MA) for about 3 minutes

8. Rinse with IPA and DI water, and dry with N_2 gas

B.4. Pneumatic Layer Master Fabrication Procedure

1. Rinse a bare 3 inch silicon wafer with acetone, IPA, and DI water in sequence, and dry with N_2 gas

2. Dehydrate baking at 200 ℃ for 10 minutes

3. Spin coat 120 μm thick photoresist (SU-8™ 2050, Microchem, Inc., Newton, MA) on the pre- pattered silicon wafer at 800 rpm for 40 seconds

4. Soft baking at 65 ℃ for 10 minutes, followed by 95 ℃ baking for 45 minutes, cool down

5. Expose UV using a mask aligner (MA6, SUSS MicroTec Inc., Waterbury Center, VT) at 250 mJ/cm^2 with the pneumatic layer photomask

6. Post exposure baking at 65 ℃ for 10 minutes, followed by 95 ℃ baking for 40 minutes, cool down

7. Develop the patterns using Microposit Thinner Type P (Shipley Co., Marlborough, MA) for about 5 minutes

8. Rinse with IPA and DI water, and dry with N_2 gas

APPENDIX C

PDMS DEVICE FABRICATION PROCEDURE

C.1. Fluidic Layer PDMS Membrane Fabrication Procedure

1. Place the fabricated fluidic layer master mold wafers inside the desiccator together with a weight boat containing 6 ~ 7 drops of tridecafluoro-1,1,2,2-tetrahydrooctyl (trichlorosilane, United Chemical Technologies, Inc., Bristol, PA)

2. Vacuum the desiccator for 10 min to allow trichlorosilane vaporize and evenly sprayed over the wafers

3. Mix PDMS (Sylgard® 184, Dow Corning, Inc., Midland, MI) prepolymer with curing agent at 10 : 1 ratio, and degas in a desiccator for 10 minutes

4. Pour the degassed PDMS prepolymer mixture onto trichlorosilane coated master wafers for 3 g per 3 inch wafer, and degas again in the desiccator for 10 min

5. Spin coat at 700 rpm for 30 seconds

6. Cure in an 85 ℃ oven for 2 h

C.2. Pneumatic Layer PDMS Block Fabrication Procedure

1. Place the fabricated pneumatic layer master mold wafers inside the desiccator together with a weight boat containing 6 ~ 7 drops of tridecafluoro-1,1,2,2-tetrahydrooctyl (trichlorosilane, United Chemical Technologies, Inc., Bristol, PA)

2. Vacuum the desiccator for 10 min to allow trichlorosilane vaporize and evenly sprayed over the wafers

3. Mix PDMS (Sylgard® 184, Dow Corning, Inc., Midland, MI) prepolymer with curing agent at 10 : 1 ratio, and degas in a desiccator for 10 minutes

4. Pour the degassed PDMS prepolymer mixture onto trichlorosilane coated master wafers for 20 g per 3 inch wafer, and degas again in the desiccator for 30 min

5. Cure in an 85 ℃ oven for 2 h

C.3. PDMS Device Bonding

1. Peel off the cured PDMS fluidic layer membrane and pneumatic layer block

2. Punch holes in the pneumatic layer block with a gauge 19 needle

3. Open via holes on the fluidic layer membrane with a sharp tweezer

4. Apply oxygen plasma treatment (100 mTorr, 100W, 40 sec) for both fluidic layer membrane and pneumatic layer block, visually align under a stereo microscope

5. Bake on a 80 ℃ hotplate for 8 h

APPENDIX D

CELL CULTURE PROTOCOL

D.1. Materials and Reagents

[HCT116-MKI67-1000 GFP] (RPMI 1640)
1 L: RPMI 1640 medium: RPMI 1640 (Invitrogen, Catalog number: 11875-085) with 10% Fetal Bovine Serum (Invitrogen, Catalog number: 16000-044), 20 mM HEPES (Invitrogen, Catalog number: 15630-080), 2-4 mM additional L-Glutamine and 100 units/ml of Penicillin/Streptomycin (equivalent to 10ml Penicillin-Streptomycin-Glutamine (100X), liquid, Invitrogen, Catalog number: 10378-016)
(all given numbers are the final concentration)

[H4IIE] (ALPHA-MEM)
500 ml: 5 g MEM/ALPHA (Thermo Scientific Hyclone, Catalog number: SH30007.03), added into 425 ml ultrapure water from Milli-Q water purification system (Millipore), 1.755 g D-glucose (Fisher Scientific, Catalog number: BP350-1), 1.1 g Sodium Bicarbonate for 5% CO2 (VWR, Catalog number: 12001-650), 50 ml Fetal Bovine Serum (Invitrogen, Catalog number: 16000-044), 10 ml Pen-Strep (Fisher Scientific, Catalog number: SV30010), adjust pH to 7.3 with HCl/NaOH, filter with Steritop filters (Millipore, Catalog number: SCGPT05RE)

0.05% Trypsin-EDTA (1x), phenol red (Invitrogen, Catalog number: 25300-054)
PBS (Invitrogen, Catalog number: 10010-023)
70% Ethanol in water

D.2. Equipments

Clean 37 ℃ water bath

Personal protective equipment (sterile gloves, laboratory coat, safety goggle)

Biosafety Cabinet Class II

37 ℃ and 5% CO_2 Incubator

Aspirator, centrifuge, pipette

D.3. Procedure

1. Here HCT116-MKI67-1000 GFP cell line is used as an example, for H4IIE cells the general procedures are the same while the medium need to be changed to ALPHA-MEM.
2. Warm PRMI 1640 medium and trypsin-EDTA in the 37 ℃ water bath for about 15 min, and turn on the centrifuge machine ahead if cooling function is included. Label the centrifuge tube and new culture flask as below:

HCT116-MKI67-1000 GFP
09/09/2011
HAN

3. For a T25 culture flask, remove old medium with aspirator
   (cap the glass tip with disposable 10 µl pipet tips for each use)
4. Pipet 5 ml PBS (for T75 flask and petri dish, use 10 ml) gently into the T25 flask, gently shake for 30 s
5. Remove PBS with aspirator, and add in 1 ml trypsin-EDTA (for T75 and petri dish use 2 ml). Keep the culture flask in the incubator for about 5 min
6. Observe the cell detaching under the microscope, after this process finishes wash the cell suspension with 4 ml of medium (for T25 and petri dish 8 ml is needed to reach 10 ml of final volume) and transfer the solution into 15 ml centrifuge tube

7. Centrifuge at 800-1000 rpm for 4:30 min to 5min (higher rpm and longer centrifuge would increase cell aggregation). For centrifuges without cooling function, the centrifuge holders need to be kept in the 4 ℃ refrigerator. For centrifuges with cooling function, the centrifuge needs to be pre-cooled. This is to reduce cell adhesion to sidewall and enhance cell pellet separation from basal medium
8. Remove the supernatant with the aspirator. Add 5 ml RPMI1640 medium to the new T25 culture flask and resuspend the cell pellets to 2 ml in fresh medium. Split the cell suspension at 1:6–1:8 ratio to the new culture flask
9. Keep the cells in a 37 ℃ and 5% CO_2 incubator

APPENDIX E

CELL STAINING PROTOCOL

E.1. Materials and Reagents

[HCT116-MKI67-1000 GFP] (RPMI 1640)
1 L: RPMI 1640 medium: RPMI 1640 (Invitrogen, Catalog number: 11875-085) with 10% Fetal Bovine Serum (Invitrogen, Catalog number: 16000-044), 20 mM HEPES (Invitrogen, Catalog number: 15630-080), 2-4 mM additional L-Glutamine and 100 units/ml of Penicillin/Streptomycin (equivalent to 10ml Penicillin-Streptomycin-Glutamine (100X), liquid, Invitrogen, Catalog number: 10378-016)
(all given numbers are the final concentration)

0.05% Trypsin-EDTA (1x), phenol red (Invitrogen, Catalog number: 25300-054)
PBS (Invitrogen, Catalog number: 10010-023)
70% Ethanol in water
Centrifuge tubes (Corning®, Catalog number: 430052)
T25 Cell culture flask (BD Falcon™, Catalog number: 353108)
Vybrant® DyeCycle™ Violet stain *5 mM in water (Invitrogen, Catalog number: V35003)
Microcentrifuge tubes (Fisher Scientific, Catalog number: 05-408-129)

E.2. Equipments

Clean 37 ℃ water bath
Personal protective equipment (sterile gloves, laboratory coat, safety goggle)
Biosafety Cabinet Class II
37 ℃ and 5% CO_2 Incubator

Aspirator, centrifuge, pipette

E.3. Procedure

1. For a T25 cell culture flask (> 90% confluency), follow the steps instructed in the cell culture protocol to prepare cell pellets from centrifuge
2. Use the aspirator to remove the supernatant. Resuspend the cell pellets to 1 ml in RPMI 1640 medium and gently pipet to allow mixing
3. Perform cell counting as instructed in the separate protocol and prepare a 1 ml cell solution microcentrifuge tube at the density of 1×10^6 cells/ml
4. Add in DyeCycle™ Violet stain at 5 μM
5. Concentrations need to be adjusted according to the fluorescence intensity measurement
6. Wrap the mixed cell stain solution tubes with aluminum and keep it in the 37℃ and 5% CO_2 incubator for 30 min. Protect from light
7. Resuspend cells into desired density and perform cell culture and analysis. To achieve higher density another step of centrifuge can be performed

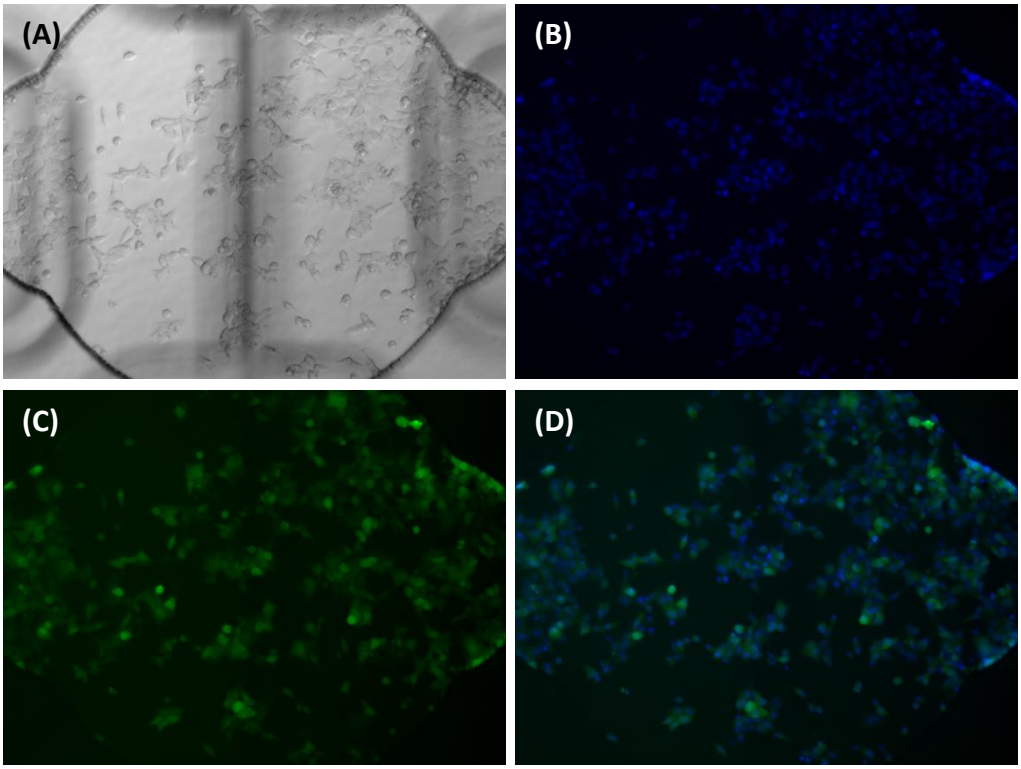

Figure E.1. HCT116-MKI67-1000 GFP cells in the microfluidic device. (A) Brightfield image of the HCT116-MKI67-1000 GFP cells seeded in the microfluidic device. (B) Blue fluorescence image of cells in (A) showing nuclei stained with DyeCycle™ Violet stain at 5 μM. (C) Green fluorescence image of the cells in (A) showing GFP reporter expression. (D) Merged image of the blue and green fluorescence channels.

APPENDIX F

OPERATION CONTROL AND DATA ACQUISITION

Device operation and data acquisition were automatically controlled by user made LabVIEW™ programs.

F.1. MICROFLUIDIC NETWORK-BASED LIVE CELL COMBINATION DRUG SCREENING PLATFORM

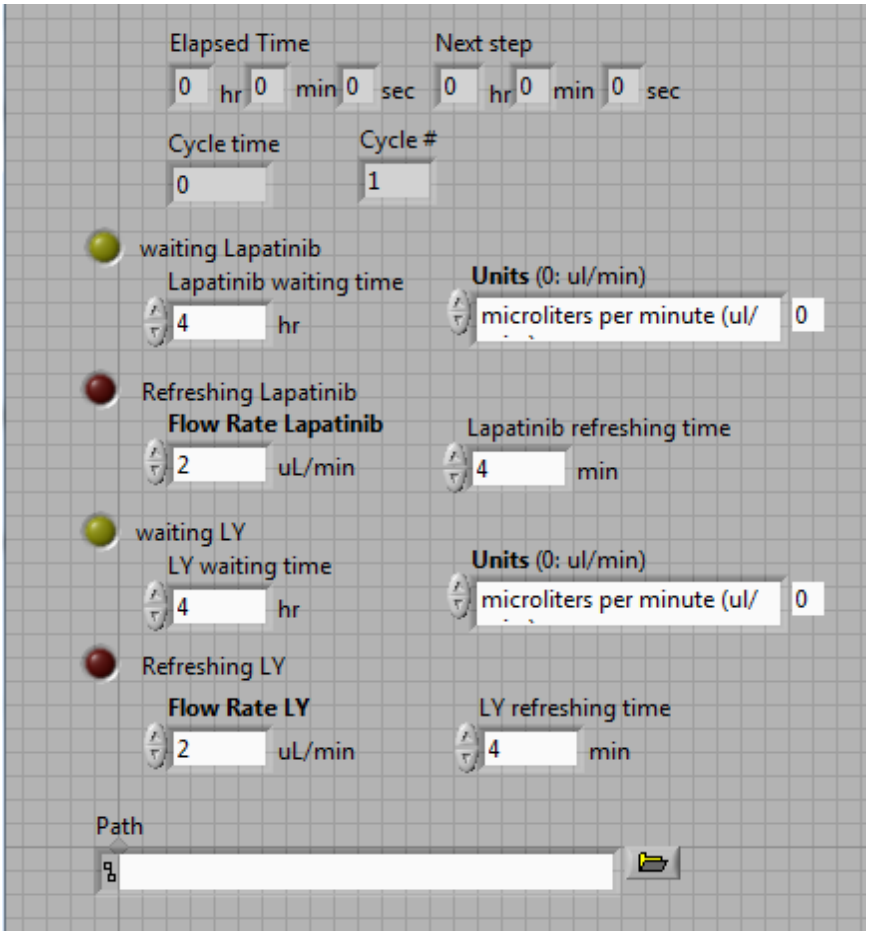

Figure F.1. Front panel of the LabVIEW™ program for microfluidic network-based combination drug screening system (2Xmas-sequential__20100410.vi)**.**

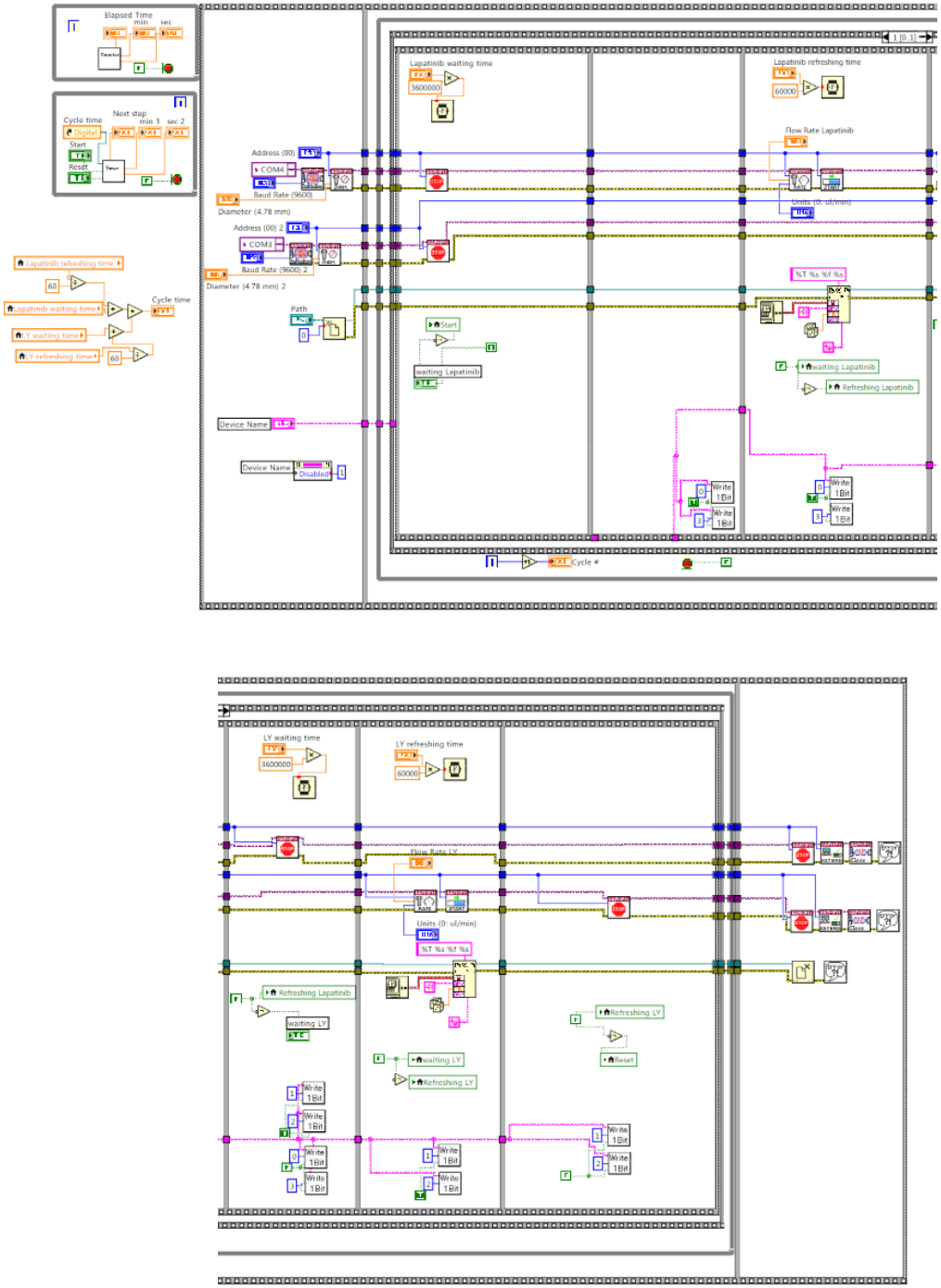

Figure F.2. Block diagram of the LabVIEW™ program for microfluidic network-based combination drug screening system (2Xmas-sequential__20100410.vi)**.**

F.2. MICROFLUIDIC GEOMETRIC METERING-BASED LIVE CELL TOXIN SCREENING PLATFORM

Figure F.3. Front panel of the LabVIEW™ program for microfluidic geometric metering-based live cell toxin screening system (Geometric toxin screeing_toxin__20110715.vi)**.**

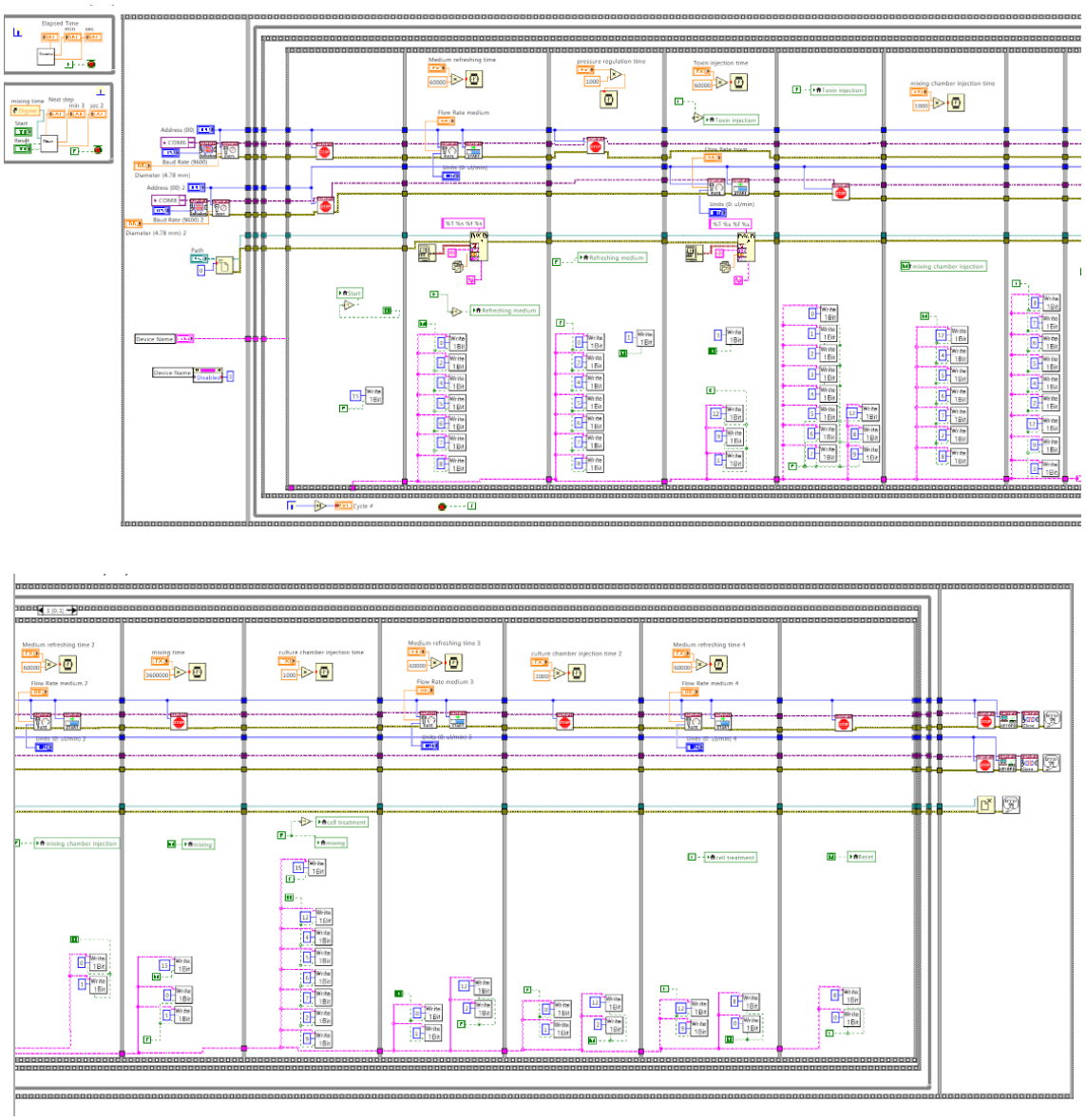

Figure F.4. Block diagram of the LabVIEW™ program for microfluidic geometric metering-based live cell toxin screening system (Geometric toxin screeing_toxin__20110715.vi)**.**

VITA

Han Wang received his Bachelor of Engineering degree in Microelectronics from Tsinghua University in 2009. He entered the Electrical Engineering program at Texas A&M University in September 2009 and received his Master of Science degree in December 2011. His research interests include development of microfluidic platforms for cancer cell biology and drug discovery, such as live cell high-throughput screening, and single cell assay. He is currently continuing his research endeavor with Dr. Arum Han at Texas A&M University as a PhD. student in the applications of microfluidic and microfabrication technologies in general cell biology with the focus on cancer metastasis and multi-mode cancer analysis.

Mr. Wang may be reached at NanoBio Systems Lab, 234F Zachry Engineering Building, Texas A&M University, College Station, TX 77843. His email is michael.wangh86@gmail.com.